

11. SITE 666¹

Shipboard Scientific Party²

HOLE 666A

Date occupied: 6 April 1986, 1515 UTC
Date departed: 7 April 1986, 1304 UTC
Time on hole: 21.75 hr
Position: 3°29.84' N, 20°10.03' W
Water depth (sea level; corrected m, echo-sounding): 4519.3
Water depth (rig floor; corrected m, echo-sounding): 4529.8
Bottom felt (rig floor; m, drill pipe measurement): 4527.3
Distance between rig floor and sea level (m): 10.5
Total depth (rig floor, m): 4677.8
Penetration (m): 150.5
Number of cores (including cores with no recovery): 16
Total length of cored section (m): 150.5
Total core recovered (m): 150.48
Core recovery (%): 100.0
Oldest sediment cored:
Depth (mbsf): 150.5
Nature: clayey nannofossil ooze
Age: early Pliocene (4.6–5.0 Ma)

Principal results: Site 666 is located in the eastern equatorial Atlantic at 3°29.84' N, 20°10.03' W, at a water depth of 4516.8 m in relatively flat terrain along the base of the southeastern margin of the Sierra

Leone Rise (see "Background and Scientific Objectives" section, this chapter). The site is situated in a region of well-stratified, flat-lying, moderately reflective layers that are partly draped over acoustic basement and also tend to have the deeper basement lows filled in (see "Background and Scientific Objectives" section, this chapter). Our primary objective was to obtain a Pliocene–Pleistocene sequence for use as part of a depth transect to study deep-water isolation in the eastern equatorial Atlantic. A secondary objective was to use this set of cores for monitoring (1) long-term fluxes in CaCO₃ and other pelagic components from surface waters, (2) CaCO₃ dissolution, and (3) downslope redistribution.

From Hole 666A, we recovered a total of 16 advanced piston corer (APC) cores taken continuously to a depth of 150.48 meters below seafloor (mbsf) (Table 1). Recovery averaged 100.0% from Hole 666A. Coring was terminated after only one hole because of extensive turbidites.

Site 666 consists of two lithologic units. Unit I (0–141 mbsf) consists of upper Pliocene to Pleistocene (4.1–0 Ma) nannofossil oozes, foraminifer-nannofossil oozes, and siliceous-nannofossil oozes. Secondary lithologies include muddy and mud- and clay-bearing nannofossil oozes (Fig. 1). CaCO₃ values vary between 70% and 90%, except at 0 to 27 mbsf, where more abundant biogenic (diatom) opal coincides with CaCO₃ minima as low as 0% (see "Organic Geochemistry" section, this chapter). The upper 27 m represents the last 1.5 m.y. Organic carbon shows an increase near 80 mbsf (~2.5 Ma) and 12 mbsf (0.5 Ma).

Lithologic Unit II (141–150.48 mbsf) is composed of lower Pliocene (and possibly upper Miocene) clay-bearing nannofossil ooze and silt-bearing, clayey nannofossil ooze. CaCO₃ values decline progressively from 90% to 40% toward the bottom of the cored interval (see "Organic Geochemistry" section, this chapter). This unit appears to be the top of the red clay lithology observed at Site 665.

Pelagic sequences are interrupted by numerous turbidites that consist mostly of redistributed foraminifer-rich pelagic sediments. About 50% (75 m) of the Pliocene–Pleistocene sediment in Hole 666A is turbidite-deposited, and every core contains one or more turbidite units. Several sharp, unburrowed contacts, possibly indicative of erosion by bottom currents, also are scattered throughout the sequence.

Paleomagnetic stratigraphy gave usable datum levels down to the Gauss chron (see "Paleomagnetism" section, this chapter) in the pelagic sequences between turbidites. Several of the shorter magnetic subchrons were not found, perhaps because of erosion. Both nannofossils and planktonic foraminifers (moderately dissolved) provided numerous additional datum levels. Diatoms were virtually absent, except in the top three cores.

With the turbidite sequences removed, the pelagic depositional rates average 16 to 20 m/m.y. in the interval 0–3.9 Ma (see "Sediment-Accumulation Rates" section, this chapter). This is about equivalent to, or slightly less than, the pelagic deposition rate at Site 665, where only a few late-Pliocene turbidites disrupted the pelagic sequence. Below 3.9 Ma, pelagic rates are less than 10 m/m.y., but the exact rate is not constrained well by the few available datum levels.

Paleoclimatic interpretations of the record at Site 666 are limited by common turbidites and by uncertainties when determining the tops of the turbidite units in the layers with finer grain sizes. Several tendencies noted at previous Leg 108 sites again are evident at Site 666, particularly the late Pliocene to Pleistocene trend toward larger-amplitude CaCO₃ changes, higher opaline silica (diatom) contents, and more organic carbon (Fig. 1). These tendencies all suggest some combination of increasing silica productivity, increasing terrigenous dilution, decreasing carbonate productivity, or increasing carbonate dissolution throughout the late Pliocene to Pleistocene.

¹ Ruddiman, W., Sarnthein, M., Baldauf, J., et al., 1988. *Proc., Init. Repts. (Pt. A), ODP*, 108.

² William Ruddiman (Co-Chief Scientist), Lamont-Doherty Geological Observatory, Palisades, NY 10964; Michael Sarnthein (Co-Chief Scientist), Geologisch-Paläontologisches Institut, Universität Kiel, Olshausenstrasse 40, D-2300 Kiel, Federal Republic of Germany; Jack Baldauf, ODP Staff Scientist, Ocean Drilling Program, Texas A&M University, College Station, TX 77843; Jan Backman, Department of Geology, University of Stockholm, S-106 91 Stockholm, Sweden; Jan Bloemendal, Graduate School of Oceanography, University of Rhode Island, Narragansett, RI 02882-1197; William Curry, Woods Hole Oceanographic Institution, Woods Hole, MA 02543; Paul Farrimond, School of Chemistry, University of Bristol, Cantocks Close, Bristol BS8 1TS, United Kingdom; Jean Claude Faugeres, Laboratoire de Géologie-Océanographie, Université de Bordeaux I, Avenue des Facultés, Talence 33405, France; Thomas Janacek, Lamont-Doherty Geological Observatory, Palisades, NY 10964; Yuzo Katsura, Institute of Geosciences, University of Tsukuba, Ibaraki 305, Japan; Hélène Manivit, Laboratoire de Stratigraphie des Continents et Océans, (UA 319) Université Paris VI, 4 Place Jussieu, 75230 Paris Cedex, France; James Mazzullo, Department of Geology, Texas A&M University, College Station, TX 77840; Jürgen Mienert, Geologisch-Paläontologisches Institut, Universität Kiel, Olshausenstrasse 40, D-2300 Kiel, Federal Republic of Germany, and Woods Hole Oceanographic Institution, Woods Hole, MA 02543; Edward Pokras, Lamont-Doherty Geological Observatory, Palisades, NY 10964; Maureen Raymo, Lamont-Doherty Geological Observatory, Palisades, NY 10964; Peter Schultheiss, Institute of Oceanographic Sciences, Brook Road, Wormley, Godalming, Surrey GU8 5UG, United Kingdom; Rüdiger Stein, Geologisch-Paläontologisches Institut, Universität Giessen, Senckenbergstrasse 3, 6300 Giessen, Federal Republic of Germany; Lisa Tauxe, Scripps Institution of Oceanography, La Jolla, CA 92093; Jean-Pierre Valet, Centre des Faibles Radioactivités, CNRS, Avenue de la Terrasse, 91190 Gif-sur-Yvette, France; Philip Weaver, Institute of Oceanographic Sciences, Brook Road, Wormley, Godalming, Surrey GU8 5UG, United Kingdom; Hisato Yasuda, Department of Geology, Kochi University, Kochi 780, Japan.

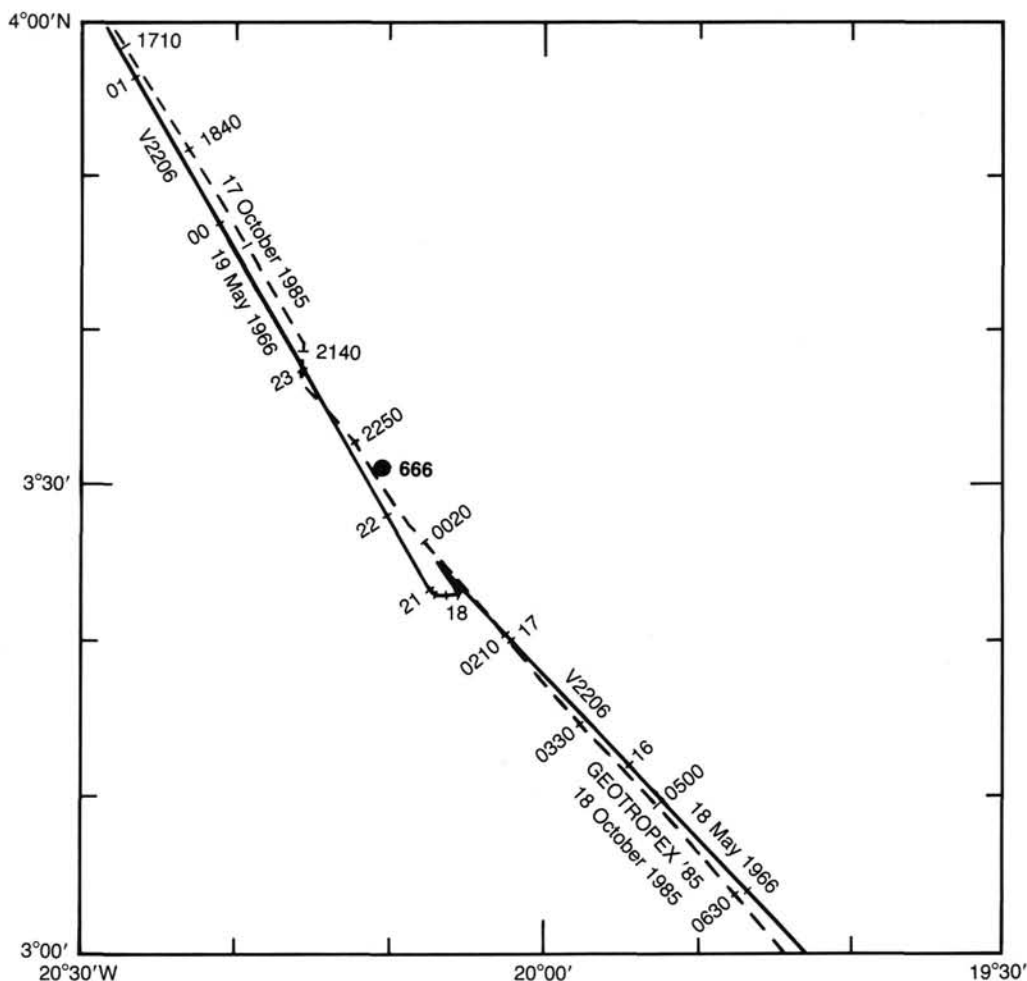


Figure 1. Seismic track lines near Site 666. The approaching track of the *JOIDES Resolution* from the southeast top to Site 666 is not shown; this track follows closely the V2206 and GEOTROPEX '85 cruise tracks.

Table 1. Site 666 coring summary (drilling depths).

Core no.	Date (April 1986)	Time (UTC)	Depths (mbsf)	Length cored (m)	Length recovered (m)	Recovery (%)
108-666A-1H	6	1847	0-8.0	8.0	8.2	102.0
108-666A-2H	6	2000	8.0-17.5	9.5	9.7	102.0
108-666A-3H	6	2117	17.5-27.0	9.5	9.8	103.0
108-666A-4H	6	2216	27.0-36.5	9.5	8.8	92.1
108-666A-5H	6	2316	36.5-46.0	9.5	9.4	98.8
108-666A-6H	7	0030	46.0-55.5	9.5	9.6	101.0
108-666A-7H	7	0140	55.5-65.0	9.5	9.0	94.5
108-666A-8H	7	0250	65.0-74.5	9.5	9.4	98.5
108-666A-9H	7	0340	74.5-84.0	9.5	9.7	101.0
108-666A-10H	7	0445	84.0-93.5	9.5	9.6	101.0
108-666A-11H	7	0605	93.5-103.0	9.5	9.6	101.0
108-666A-12H	7	0725	103.0-112.5	9.5	9.2	96.7
108-666A-13H	7	0840	112.5-122.0	9.5	9.4	98.5
108-666A-14H	7	1010	122.0-131.5	9.5	9.6	101.0
108-666A-15H	7	1120	131.5-141.0	9.5	9.7	102.0
108-666A-16H	7	1304	141.0-150.5	9.5	10.0	105.0

BACKGROUND AND SCIENTIFIC OBJECTIVES

Site 666 (target Site Eq-5) is one of four sites in a transect taken at different depths down the southern margin of the Sierra Leone Rise (see Fig. 2, "Background and Scientific Objectives" section, Site 665 chapter). We planned two major kinds of objectives at Site 666: one kind was part of the depth tran-

sect, and the other focused on broader paleoceanographic objectives.

The depth-related objectives were as follows:

1. To determine the late Neogene history of relative isolation of eastern Atlantic deep waters, based on depletion of $\delta^{13}C$ ratios and on the organic-carbon content (for a more complete discussion see "Background and Scientific Objectives" section, Site 665 chapter). For this purpose, Site 666 lies below the 3800-m water depth at which relative isolation of the eastern Atlantic deep circulation becomes evident. Together with Site 665, at a deeper water depth, Site 666 should provide control on past depth gradients in $\delta^{13}C$.

2. To assess late Neogene changes (1) in the flux of biogenic opal, organic carbon, and $CaCO_3$ from the surface waters, (2) in dissolution of $CaCO_3$ by deep waters, and (3) in redistribution of all sediment components by bottom currents.

Broader paleoenvironmental objectives at Site 666 were the following:

1. To measure late Neogene fluxes of eolian dust and fresh-water diatoms as indicators of continental source-area aridity and of wind strength.

2. To obtain a high-quality Neogene section for detailed biostratigraphic and paleomagnetic studies.

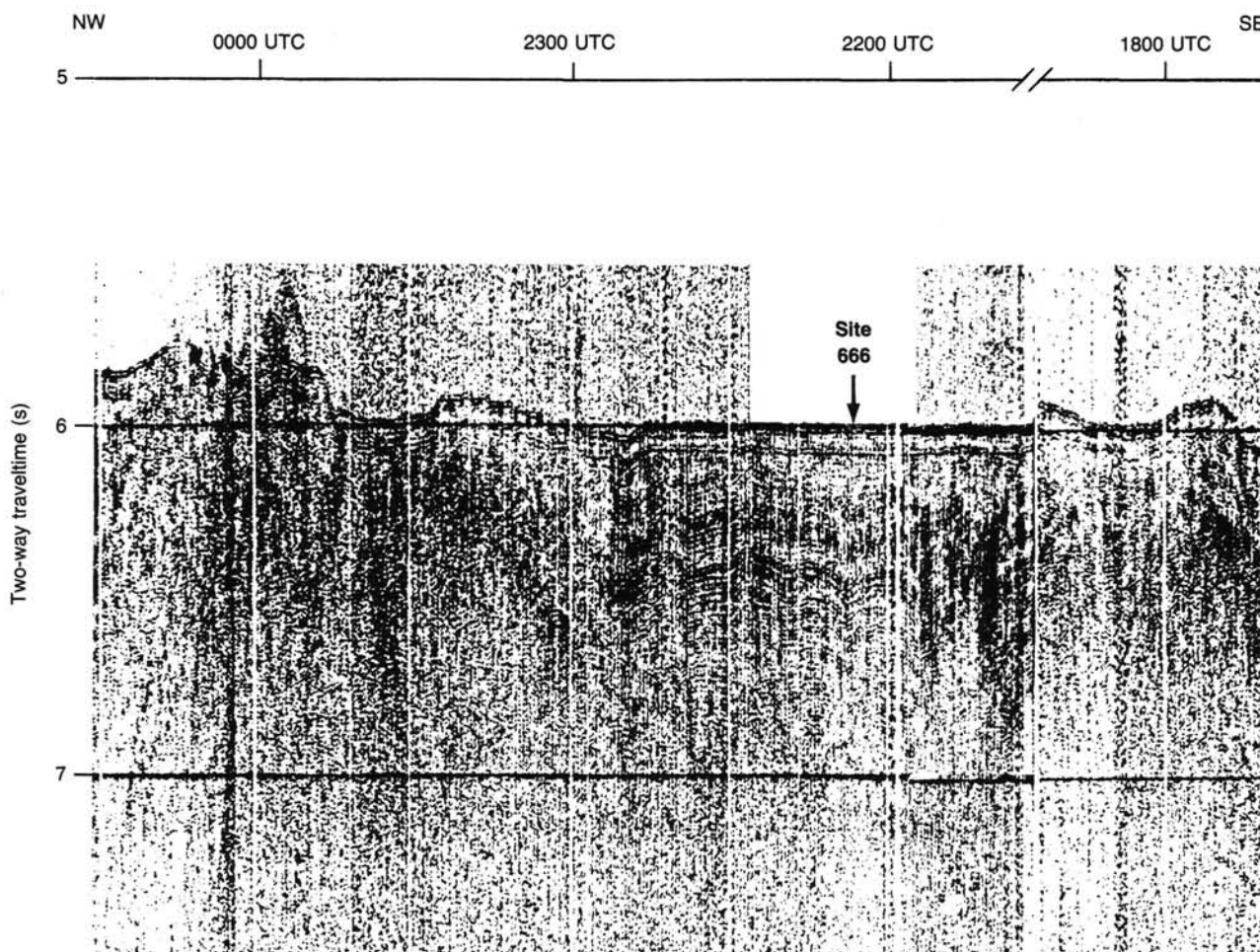


Figure 2. Seismic-reflection records from cruise V2206 near Site 666.

Geologic and Topographic Setting

Site 666 is located in the eastern equatorial Atlantic in relatively level terrain along the base of the southeastern margin of the Sierra Leone Rise (Fig. 2). Air-gun records from this region show at least 0.8 s of sediment above the acoustic basement (Figs. 3 and 4), although this basement is obscured in the immediate vicinity of Site 666 because of thick sedimentary cover. Seismic reflectors are well stratified and moderately reflective. Sediment thicknesses vary with basement relief, suggesting some net infilling of the low relief, similar in degree to that observed at Site 665.

The basement age at Site 666 is Cretaceous (about 80 Ma), based on the regional magnetic lineations and on previous drilling results. The sediment section in the upper 150 m is lower Pliocene to Holocene nannofossil ooze overlying (early) lower Pliocene and older red clay.

OPERATIONS

After departing Site 665 on 5 April 1986, we immediately streamed out our geophysical gear (80-in.³ water guns and a magnetometer) at 1750 UTC and headed for Site 666 at a speed of 5 kt, along a course of 313°. Our positions during this survey were determined by dead reckoning and occasional satellite fixes (All times are UTC, Universal Time Coordinated, formerly expressed as GMT, Greenwich Mean Time.) We continued on this course until 0413 on 6 April, then turned to a course of 150° at a point located at approximately 3°40'N, 20°18'W. We ad-

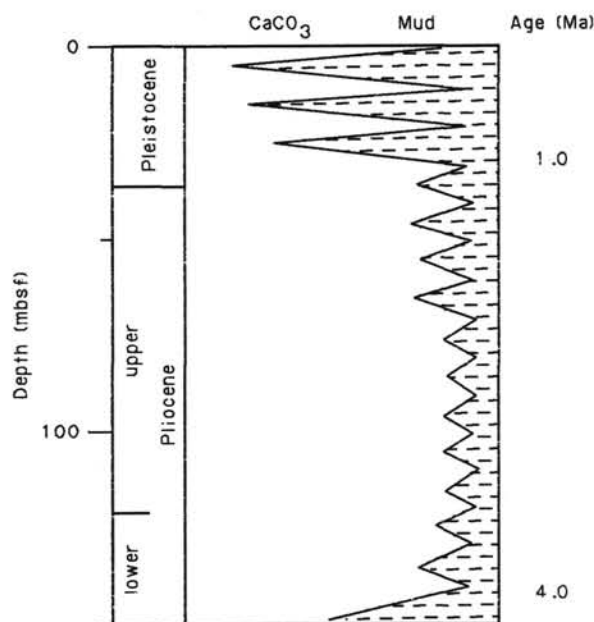


Figure 3. Biostratigraphic and lithostratigraphic summary of Hole 666A. Schematic CaCO_3 cycles indicate increased amplitude of variations from late Pliocene to late Pleistocene. Timing of change in cycles is not well constrained by limited shipboard sampling.

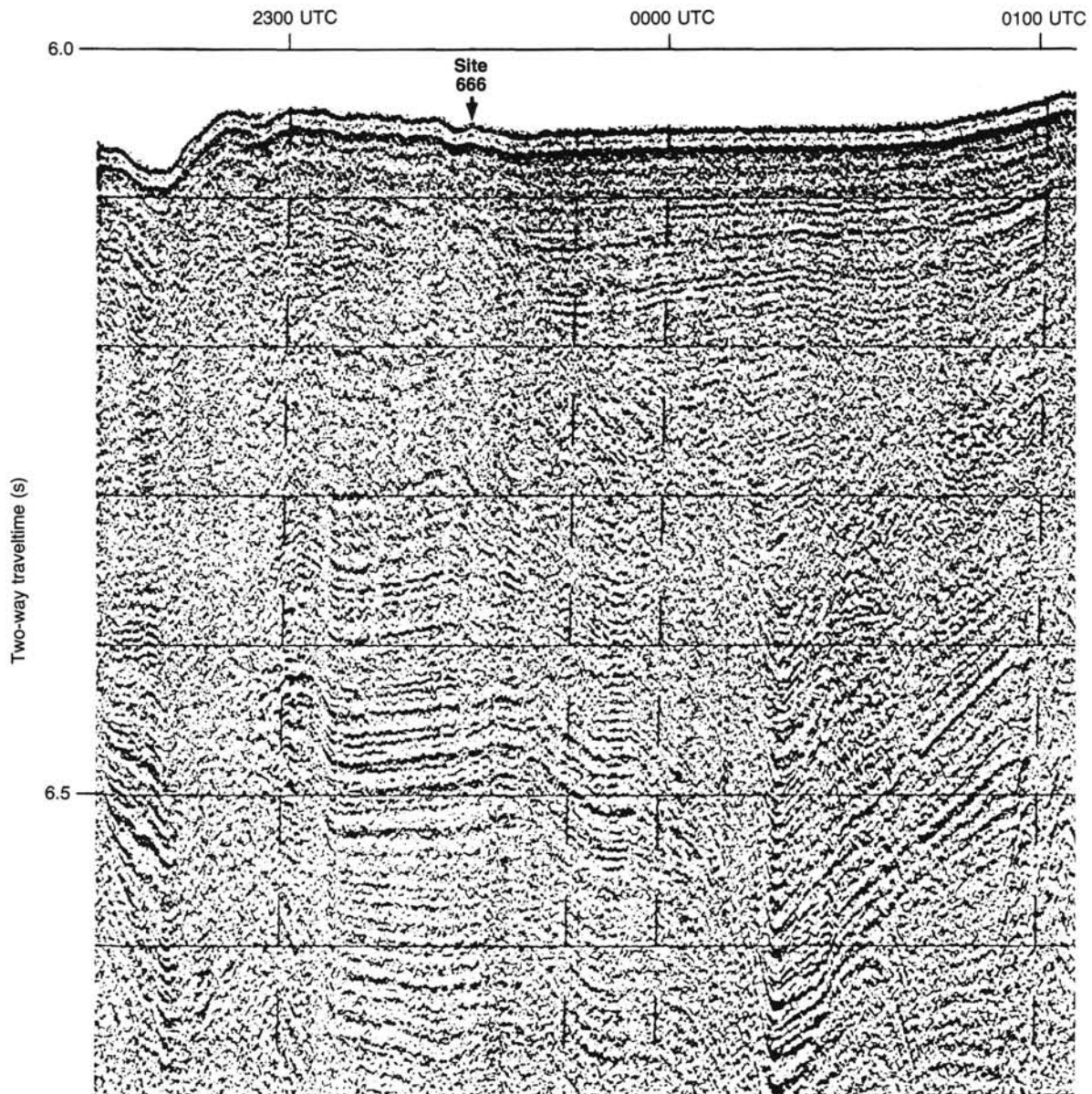


Figure 4. High-resolution, seismic-reflection record near Site 666 from GEOTROPEX '85 cruise of the *Polarstern*.

justed this course to 166° at 0642, based on a new satellite fix. At 0724, at a position of approximately $3^\circ 27.8' N$, $20^\circ 09.6' W$, we came around to a course of 353° and followed that to the location of Site 666 at $3^\circ 29.84' N$, $20^\circ 10.3' W$.

We dropped a beacon at 0745 on 6 April 1986, pulled in our geophysical gear, and returned to the beacon. We began running drill pipe into Hole 666A at 0835 and finished by 1515. Retrieval of the first good core was delayed between 1600 and 1700 because of overheating of the electronics in the core-winch shed on a hot, sunny day with no wind. In addition, our first attempt at coring the mud line resulted in a water core that was shot at a water depth of 4517 m. Finally, Core 108-666A-1H came on deck at 1847 and established the mud line at a water depth of 4516.8 m. We continued advanced piston corer (APC) coring until the final APC core (108-666A-16H) came on deck at 1304 on 7 April. Recovery from Hole 666A averaged 100.0%.

Because the sediment sequence in Hole 666A contained numerous turbidite sands that interrupted the pelagic sequence on

which our main objectives were based, we decided to cancel the offset hole and to proceed directly to Site 667. We began pulling out of Hole 666A at 1304 on 7 April, and the drill string was back on deck by 2115, at which time we got under way to Site 667 at 13 kt. The weather at Site 666 was warm and pleasant, with negligible swell.

LITHOSTRATIGRAPHY AND SEDIMENTOLOGY

Introduction

Two major stratigraphic units are recognized at Site 666 (Fig. 5). Unit I is composed of nannofossil, foraminifer-nannofossil, and siliceous-nannofossil pelagic oozes of early Pliocene and Pleistocene age (0–4.1 Ma) interbedded with numerous foraminifer sand turbidites. Unit II is composed of nannofossil and clayey nannofossil oozes of early Pliocene age (4.1–5.0 Ma) and possibly older. Each sedimentary unit is described in detail.

Unit I

Cores 108-666A-1H through -666A-15H, CC; depth, 0-141 mbsf; age, early Pliocene to Pleistocene (4.1-0 Ma).

Unit I is composed of nannofossil ooze, foraminifer-nannofossil ooze, and siliceous-nannofossil ooze interbedded throughout with numerous small and large foraminifer sands, probably with a turbidite origin. Mud- and clay-bearing and muddy nannofossil oozes are less common. Biogenic opal occurs only in the upper three cores (0-27 mbsf). The unit varies in color from pale brown, very pale brown, and light yellowish brown to reddish yellow. Nannofossil and siliceous oozes that are rich in organic carbon are generally dark gray. Below 27 mbsf, the colors are generally light gray, olive gray, or white. Numerous turbidites interrupt the pelagic deposits throughout this unit. Large turbidites (greater than 6 m thick) are found in Cores 108-666A-5H, -666A-7H, and -666A-9H.

The carbonate content of this unit varies from near 0% to greater than 80% (Fig. 5). Low carbonate values are found in the upper 27 m of the section. Lower carbonate values coincide with increased percentages of biogenic silica. Diatoms are the primary biogenic opal component, although radiolarians also are present in minor amounts. The primary terrigenous components are clay (up to 35%), accessory minerals, and quartz. Organic carbon increases from negligible values to greater than 1% by weight above 10 mbsf.

Unit II

Sections 108-666A-16H-1 through -666A-16H, CC; depth, 141-150 mbsf; age, Miocene(?) to early Pliocene (5(?) - 4.1 Ma).

Unit II is composed of white to pale yellow, clay-bearing nannofossil ooze and pale brown, light yellowish brown, or yellowish brown, silt-bearing, clayey nannofossil ooze. Graded bed-

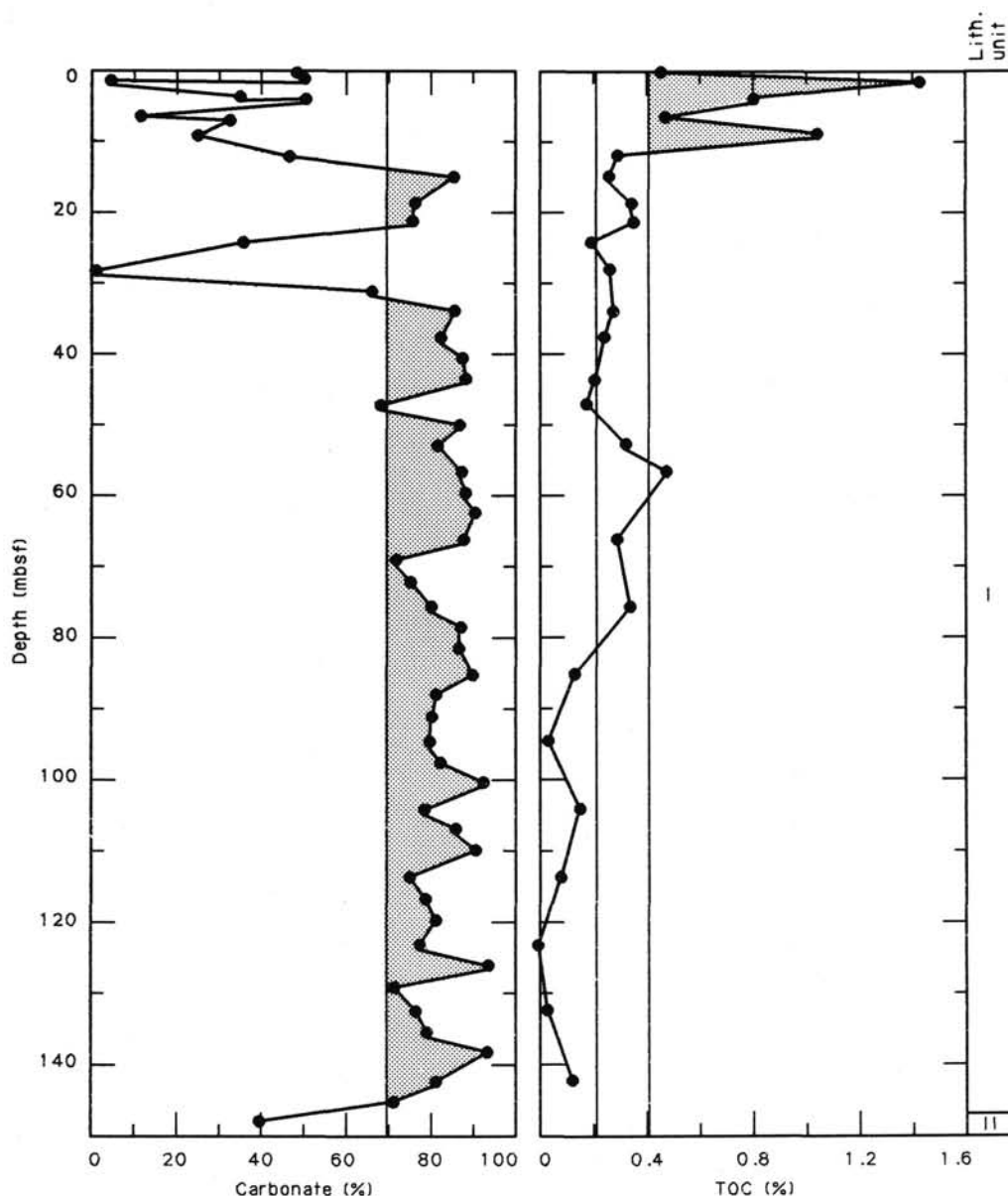


Figure 5. Percentages of carbonate and total-organic-carbon data plotted vs. depth below seafloor for Hole 666A.

ding and sharp lower contacts are common. Foraminifers are generally absent or rare in the pelagic deposits, but are quite common in the turbidites. Accessory minerals are an important component of the terrigenous fraction, while clay concentrations reach 25%. This unit appears to correlate with the top of Unit II at Site 665.

Depositional History

The depositional history of Site 666 reflects pelagic deposition, interrupted frequently by turbidite deposition. Before 4.1 Ma, this site was located near the carbonate compensation depth (CCD). Nannofossil oozes rich in clay, but generally without foraminifers, were deposited by pelagic processes. These deposits were interbedded with rapidly deposited foraminifer turbidites. Between 4.1 Ma and approximately 1.5 Ma, the pelagic deposits were generally foraminifer-nannofossil oozes and nannofossil oozes with variable clay concentrations. After that time, biogenic opal productivity in the surface water increased, and deposition of the biogenic opal fraction continued throughout the late Pleistocene. Organic-carbon preservation in these sediments increased at approximately 2.5 Ma, correlating with a similar increase at Site 665. Throughout the entire record at Site 666, turbidite deposition dominated the sedimentary processes. Based on a rough correlation of Unit II at this site with Unit II at Site 665, approximately 75 m of additional sediment (mostly foraminifer sand) was delivered to Site 666 by gravity processes.

BIOSTRATIGRAPHY

Site 666 makes up part of a depth transect across the southern flank of the Sierra Leone Rise. This site was drilled in a water depth of 4516.8 m and consists of a single hole, Hole 666A, which was cored to a depth of 150.5 mbsf, and which extends back to the lower Pliocene (Fig. 6). Calcareous nannofossils and planktonic foraminifers are generally common to abundant, with moderate to good preservation; however, a few samples show decreased abundances and poor preservation. Benthic foraminifers are almost always present, although the assemblage varies considerably in abundance, preservation, and species composition. Diatoms are extremely sparse at this site and were absent from most samples examined.

As at 662 and 664, the sediment column at Site 666 contains large amounts of reworked material, particularly in the form of turbidites (see "Sediment-Accumulation Rates" section, this chapter). The presence of allochthonous sediment results in the juxtaposition of older microfossil assemblages above younger ones, as well as samples with a mixture of fossils of different ages. When constructing a biostratigraphic framework, we attempted to correct for the presence of these reworked sediments.

Calcareous Nannofossils

Every core recovered at Site 666 contains intervals in which the calcareous-nannofossil assemblages represent mixtures of different biostratigraphic zones. Approximately 50% of the Pliocene and Pleistocene sediments reflect pelagic deposition, with the other one-half composed of turbidites. These turbidite units vary in length from a few centimeters to about 12 m (see "Lithostratigraphy and Sedimentology" section, this chapter). We tried to exclude samples taken from turbidites, samples containing obvious reworking, or samples with no reworking, but in which assemblages of older age overlie stratigraphically younger ones. This was necessary to achieve an elementary biostratigraphical understanding of the sequence, but it diminished stratigraphic precision. Reworking is restricted to late Neogene species, except for a few observations of the middle Eocene through early Miocene species, *Cyclicargolithus floridanus*.

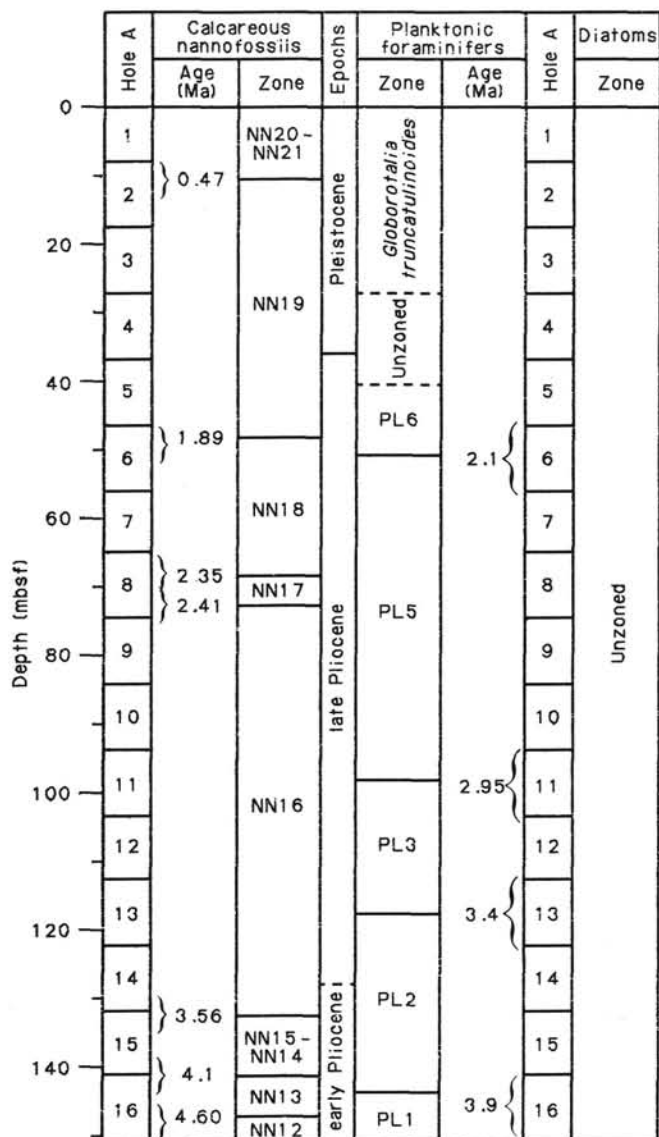


Figure 6. Zonal assignments for cores recovered from Hole 666A.

Preservation is moderate in terms of both placolith dissolution and discoaster overgrowth, except in Core 108-666A-16H, where the transition to the red-clay facies occurs. Here, dissolution is intense and also has affected the discoasters (e.g., most samples in Core 108-666A-16H show great abundances of isolated discoaster rays or fragments of rays). *Ceratolithus rugosus* and the robust *Discoaster surculus* appear least affected by dissolution, given the splendid preservation of their primary morphological features in some samples in Core 108-666A-16H. This core is also the only one displaying a decrease in overall nannofossil abundance.

Pleistocene

The disappearance of *Pseudoemiliania lacunosa* is considered to occur in Section 108-666A-2H-2; it is extremely rare in Section 108-666A-2H-1, and its common presence in the core-catcher sample of Core 108-666A-1H is caused by sediment mixing from late Pliocene sources. Samples 108-666A-4H-3, 56 cm, and -666A-4H-3, 124 cm, contained neither *Helicosphaera sellii* nor *Calcidiscus macintyreii*. The former was observed alone in

Sample 108-666A-4H-4, 140 cm, but both species were present in Sample 108-666A-4H-5, 30 cm. Thus, the interval between the last two samples appears to yield a reliable extinction event for *C. macintyreii*.

Pliocene

Section 108-666A-5H-5 contained *Discoaster brouweri* and *Discoaster triradiatus*, but approximately one-half the discoaster assemblage consisted of obviously reworked forms. Samples 108-666A-5H-6, 118 cm, and -666A-5H, CC displayed an upper Pliocene/lower Pleistocene assemblage without discoasters, whereas both *D. brouweri* and *D. triradiatus* were common in Sample 108-666A-6H-2, 110 cm. This sample also contained obviously reworked Pliocene discoasters—about 10% in relation to the sum of *D. brouweri* and *D. triradiatus*. The latter species constituted 37% relative to the former species in Sample 108-666A-6H-2, 110 cm; hence, we consider it likely that the final discoaster extinction events occurred between this sample and Section 108-666A-5H, CC. The beginning of the acme interval of *D. triradiatus* was observed between Samples 108-666A-6H-4, 110 cm, and -666A-6H-6, 90 cm.

We are less confident that we have recognized the true disappearance events of either *Discoaster pentaradiatus* or *D. surculus*, but the former is tentatively placed in Section 108-666A-8H-2 and the latter in the interval separating Sections 108-666A-8H-4 and -666A-9H-1. The disappearance of *Discoaster tamalis* may occur in Section 108-666A-9H-2, but rare occurrences throughout Core 108-666A-9H and/or reworking suggest that this event cannot be determined to better than the range between Samples 108-666A-9H-1, 110 cm, and -666A-10H-2, 140 cm.

All samples investigated from Core 108-666A-12H show severe reworking of lower Pliocene assemblages, while samples from Core 108-666A-13H display assemblages characteristic of the lower part of the upper Pliocene, i.e., those containing *D. tamalis* and *Discoaster asymmetricus* but no sphenoliths or *Reticulofenestra pseudoumbilica*. Sphenoliths disappear between Samples 108-666A-14H-1, 110 cm, and -666A-14H-5, 130 cm, whereas *R. pseudoumbilica* disappears between the latter sample and Sample 108-666A-15H-2, 30 cm. *Discoaster tamalis* is present in Sample 108-666A-15H-2, 30 cm, but not in Section 108-666A-15H-7. Thus, the short overlapping in ranges between *D. tamalis* and *R. pseudoumbilica* and the fact that sphenoliths survive *R. pseudoumbilica* for a short period of time suggest that the disappearance of the latter species represents its extinction.

Perfect specimens of *Ceratolithus rugosus* were observed in Sample 108-666A-16H-3, 90 cm, and good specimens of *Ceratolithus acutus* were observed from the red-clay facies in Section 108-666A-16H, CC, indicating that the evolutionary transition between the two species occurs in the lower one-half of Core 108-666A-16H. The presence of *C. acutus* at the very base of Hole 666A also indicates that the hole terminated in basal Pliocene sediment, between 5.0 and 4.6 Ma.

Planktonic Foraminifers

Planktonic foraminifers with good-to-moderate preservation are abundant at this site, except for Pleistocene Sections 108-666A-2H, CC and -666A-3H, CC, which have poor preservation. The fauna is tropical in nature, typically characterized by *Globigerinoides trilobus*, *Globigerinoides ruber*, *Globigerinoides sacculifer*, *Neogloboquadrina humerosa*, and *Globorotalia miocenica*. *Globorotalia inflata* and *G. punctulata* were generally rare to few. Numerous turbidites are present at Site 666, resulting in the occurrence of many reworked specimens throughout a record that extends to the early Pliocene PL1 Zone.

The *Globorotalia truncatulinoides* Zone extends to Section 108-666A-3H, CC, which was underlain by a turbidite in the core-catcher sample of Core 108-666A-4H. The next sample, 108-666A-5H, CC, belongs to the late Pliocene PL6 Zone and was the only sample identified as belonging to this zone. Zone PL5 extends from Sample 108-666A-6H-6, 115 cm, through 108-666A-10H, CC, with turbidites found in core-catcher Sections 108-666A-6H, CC, -666A-7H, CC, -666A-10H, CC, and possibly 108-666A-8H, CC. This zone is characterized by the presence of numerous *Neogloboquadrina humerosa*.

Zone PL3 was identified in Sections 108-666A-11H, CC, -666A-12H-4, 55 cm, and -666A-12H, CC, and Zone PL2 in Sections 108-666A-13H, CC, -666A-14H-7, 4 cm, and -666A-15H, CC. These zones contain common *Globorotalia menardii* and *G. trilobus*. The last sample examined (108-666A-16H, CC) was found to be barren, but a sample from the same core (108-666A-16H-3, 79 cm) contained *Globigerina nepenthes*, thus placing the PL2/PL1 zonal boundary within the first three sections of Core 108-666A-16H.

Benthic Foraminifers

Except for Section 108-666A-16H, CC, benthic foraminifers occur in all core-catcher samples examined from Hole 666A. Core-catcher Samples 108-666A-1H through -666A-8H contain rare, well-preserved specimens. Core-catcher Samples 108-666A-9H through -666A-15H contain few, moderately well-preserved specimens. Whereas the assemblage in Section 108-666A-1H, CC consists of small specimens (<0.2 mm) such as *Epistominella exigua* and unilocular forms (lagenids, oolinids, and fisurinids), the assemblage in Sample 108-666A-7H, CC is dominated by large specimens (>0.3 mm) such as *Gyroidinoides soldanii*, *Oridorsalis tener*, *Planulina wuellerstorfi*, *Siphouvigerina proboscidea*, *Uvigerina peregrina*, and *Anomalinoidea* sp. The size selectivity of the assemblages suggests sediment sorting, most likely by turbidites. With the exception of the two samples mentioned above, the core-catcher samples examined contain assemblages typical of North Atlantic Deep Water.

Diatoms

With the exception of rare specimens of freshwater *Melosira* spp. and fragments of *Ethmodiscus rex* in core-catcher Samples 108-666A-1H, -666A-2H, -666A-4H, and -666A-6H, and a single specimen of *Coscinodiscus marginatus* in Section 108-666A-1H, CC, all core-catcher samples from Hole 666A contain no diatoms.

PALEOMAGNETISM

Magnetostratigraphy

Turbidites have never been a favorite with paleomagnetists. They are avoided for various reasons, including grain size and uncertainty about the reliability of the magnetization process. Site 666 is noteworthy for its abundance of turbidites; hence, the paleomagnetic data presented here were subjected to a selection process ranging from judicious to artistic. Our philosophy was to edit out data generated by the blind, continuous-measurement procedure that came from lithologies we could not sample in the field.

To illustrate the quality of the data from Site 666, we discuss the step-by-step procedure followed for generating our final interpretation. First, all data from archive halves, measured at 3-cm intervals, were plotted on a core-by-core basis. The cores from Site 666 were not oriented. Furthermore, neither the Brunhes/Matuyama nor the Jaramillo transitions were recorded within a single core. Therefore, the directional data were interpreted in terms of polarity, based on demagnetization behavior and bio-

stratigraphic constraints. A single correction then was applied to each core so that the mean "normal" declination was 90°. The resulting data set is presented in Figure 7 without further editing. These data are highly scattered, and one might despair of a reliable interpretation. However, as we will show, the simple step of eliminating data from turbidites and core tops transforms the raw data shown in Figure 7 into a reasonable magnetostratigraphy.

Our data-selection procedure is illustrated in Figure 8. As a first step, the upper 50 cm of every core was deleted, owing to the frequency of coring disturbance in core tops. Second, data associated with coarse-grained or disturbed layers were deleted. Data from Core 108-666A-5H rejected by these criteria are shown by the hatched areas (Fig. 8).

Data from the intervening pelagic oozes are high quality, as indicated by demagnetization of discrete samples. The demagnetization curves for Site 666A samples, shown in Figure 9, suggest high stability and uncomplicated behavior. These data were

corrected with the same declination as the whole cores; north is indicated by the positive y direction.

In Figure 10 we plot the data after declination correction and the data selection/rejection process. The polarity log shows all polarity units spanning more than 40 cm. Correlation to the time scale is consistent with biostratigraphic constraints, and the depths of the boundaries are included in the "Sediment-Accumulation Rates" section (this chapter).

Magnetic Susceptibility

We measured the whole-core volume susceptibilities for Cores 108-666A-1H through 108-666A-4H at 3-cm intervals. Because of the large number of turbidites, magnetic susceptibility was not measured for Hole 666.

SEDIMENT-ACCUMULATION RATES

Sediment-accumulation rates were calculated for Hole 666A based on 16 biostratigraphic and five magnetostratigraphic events

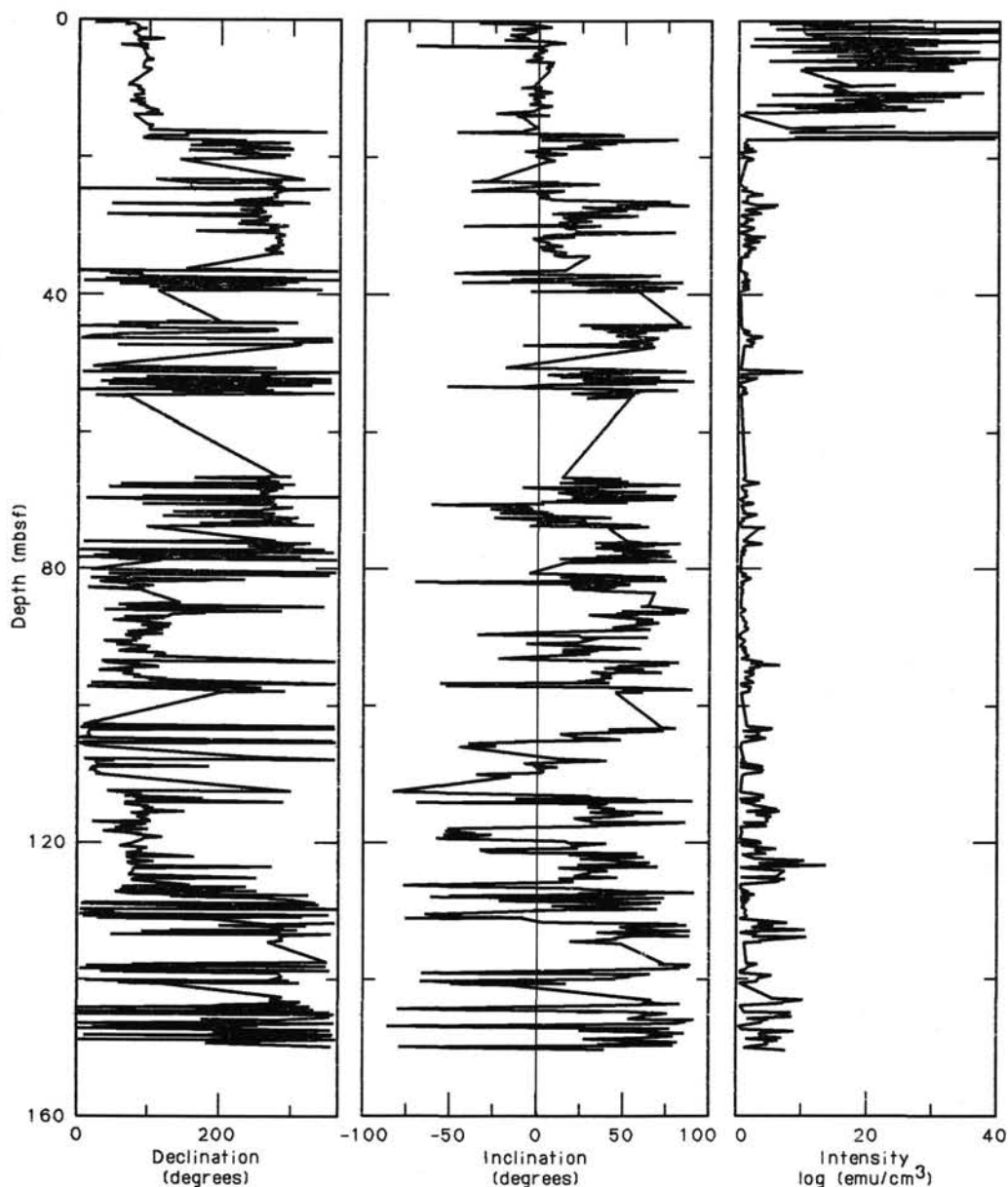


Figure 7. Declination-corrected data from archive halves for Hole 666A.

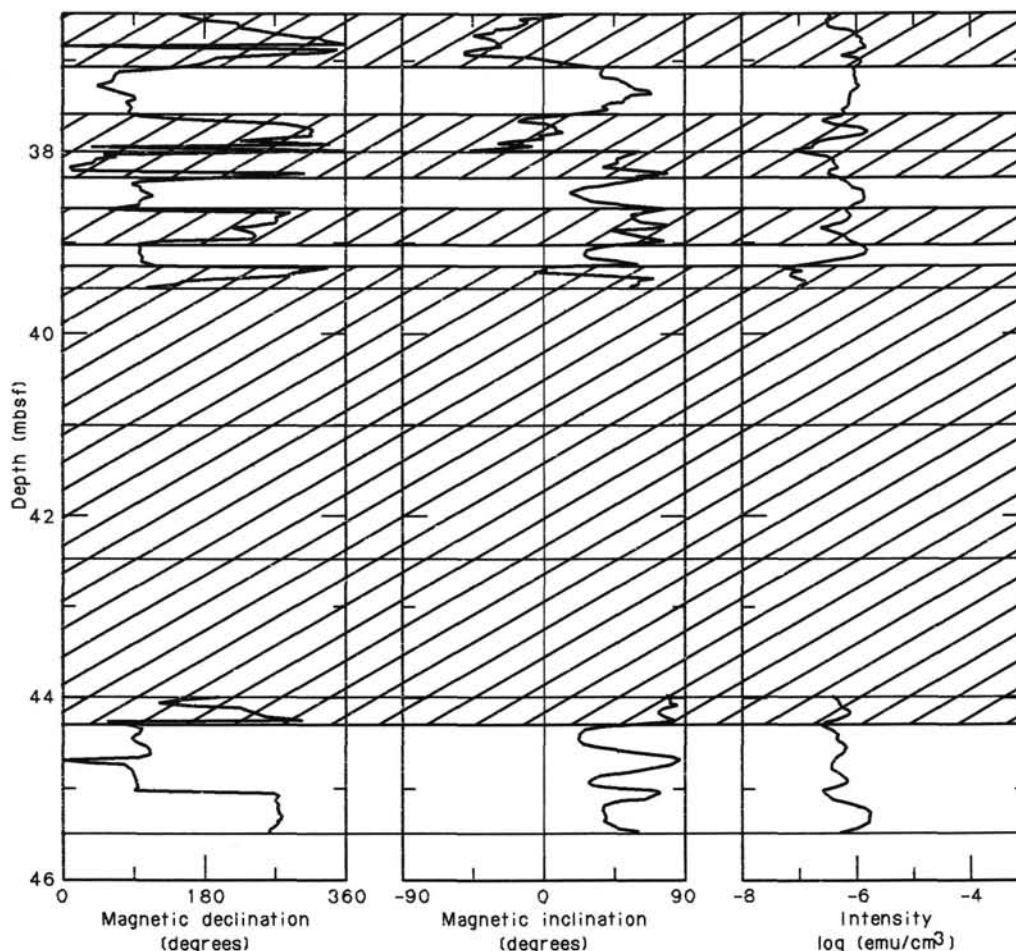


Figure 8. An example of the data-editing procedure used. Hatched areas indicate turbidite layers, and the data were deleted in these intervals.

(Table 2; Figs. 11 and 12). Because nearly one-half the section is composed of turbidites and other allochthonous sediments (see "Lithostratigraphy and Sedimentology" section, this chapter), accumulation rates based on these data would be greatly exaggerated. We have, therefore, calculated sediment-accumulation rates on a "no-turbidite/slump-free" basis (Table 3 and Fig. 12) by removing all sediments identified as allochthonous. No biostratigraphic or magnetostratigraphic event falls significantly off this corrected accumulation-rate curve.

Figure 12 reveals that, on a no-turbidite/slump-free basis, the sediment-accumulation rate has been relatively constant since the early Pliocene (3.9 Ma to the present). Since the base of the Brunhes (~0.73 Ma), sediments have accumulated at a rate of 19.5 m/m.y. Between 0.73 and 1.88 Ma, the accumulation rate was 16.4 m/m.y., and between 1.88 and 2.45 Ma, it was 18.4 m/m.y. At approximately 2.45 Ma, the accumulation-rate curve suggests improbably rapid sedimentation. We infer from this that most of the sediment between ~70 and 78 mbsf (Fig. 11) is allochthonous, even though it was not identified as such on sedimentological grounds (see "Lithostratigraphy and Sedimentology" section, this chapter).

Between ~3.9 and 2.47 Ma, the sediment-accumulation rate was 17.2 m/m.y. From the base of the section (~5.0 Ma) to ~3.9 Ma, the average accumulation rate appears to have been approximately 4.1 m/m.y. This indicates that a substantial change in the sediment-accumulation rate occurred during the late-early Pliocene, corresponding to the sedimentological change from

red clays to calcareous oozes (see "Lithostratigraphy and Sedimentology" section, this chapter).

INORGANIC GEOCHEMISTRY

Interstitial-water samples were squeezed from three sediment samples routinely recovered approximately every 50 m from Hole 666A. Values for pH and alkalinity were measured in conjunction, using a Metrohm 605 pH-meter, followed by titration with 0.1N HCl, and salinities were measured using an optical refractometer. Cl^- , Ca^{2+} , and Mg^{2+} concentrations were determined by the titrations described in Gieskes and Peretsman (1986). SO_4^{2-} analyses were conducted by ion chromatography using a Dionex 2120i instrument. Results from all analyses are presented in Table 4.

ORGANIC GEOCHEMISTRY

At Site 666, Hole 666A, 52 samples were measured for their carbonate content. Of these, 26 samples also were analyzed for total-organic-carbon (TOC) contents, and 15 samples were investigated for organic-matter type by Rock-Eval pyrolysis.

Organic and Inorganic Carbon

Inorganic carbon (IC) was determined by means of the Coulometrics Carbon Dioxide Coulometer, while total carbon (TC) was measured using the Perkin Elmer 240C Elemental Analyzer. TOC values were calculated by difference. Analytical methods are discussed, and data listed in the Appendix (this volume).

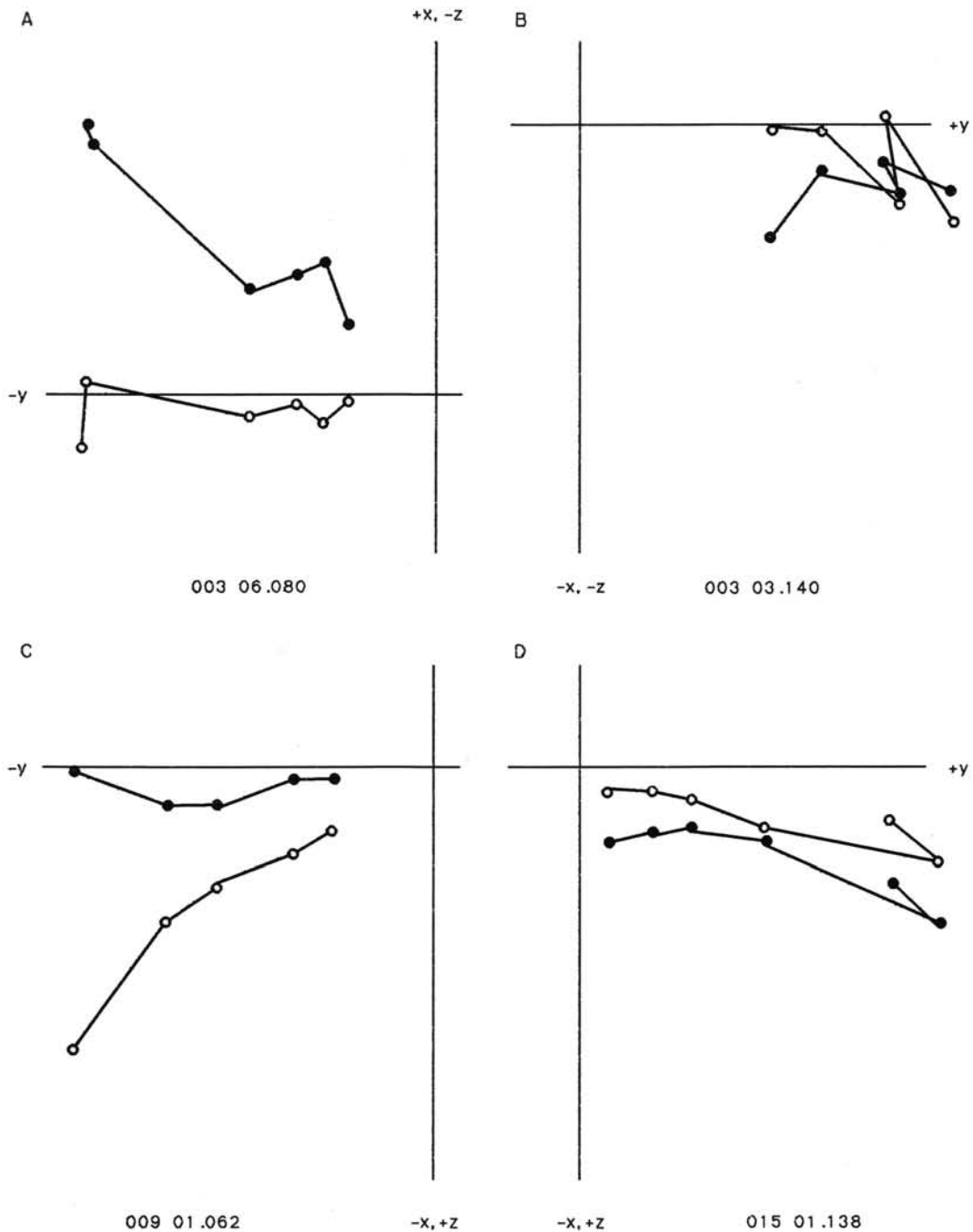


Figure 9. Vector end-point diagrams from representative samples.

According to the carbonate record, the sediment sequence at Site 666 can be divided into two parts (Fig. 13). The upper 33 mbsf (i.e., Cores 108-666A-1H through -666A-4H-3) is characterized by high-amplitude variations ranging from about 0% to 85% CaCO₃. The lower part of the sequence (i.e., Cores 108-666A-4H-4 through -666A-16H) is characterized by high carbonate values fluctuating from 70% to 94%, with one exception: the lowermost sample of the record (i.e., Core 108-666A-16H-5, 120–122 cm) has a carbonate content of about 40% (Fig. 13).

The TOC contents are relatively high in the uppermost 10 m (i.e., Cores 108-666A-1H through -666A-2H-1), ranging from 0.42% to 1.35% (Fig. 13). Below 10 mbsf down to the bottom of the hole, the TOC values are low (less than 0.4%; Fig. 13).

According to Rock-Eval results, most of the organic matter is a mixture of marine and terrigenous material (Table 5; Tissot and Welte, 1984).

Discussion

The uppermost 10 m of the sediment sequence at Site 666 is relatively enriched in (partly marine) organic carbon (0.4% to 1.35% C_{org}) and biogenic silica (see "Lithostratigraphy and Sedimentology" section, this chapter), possibly indicating periods of increased productivity. During this same interval, the decreased carbonate content may have been caused by increased carbonate dissolution and/or dilution by noncarbonate (i.e., biogenic silica and terrigenous) material. Below 10 mbsf, the sedi-

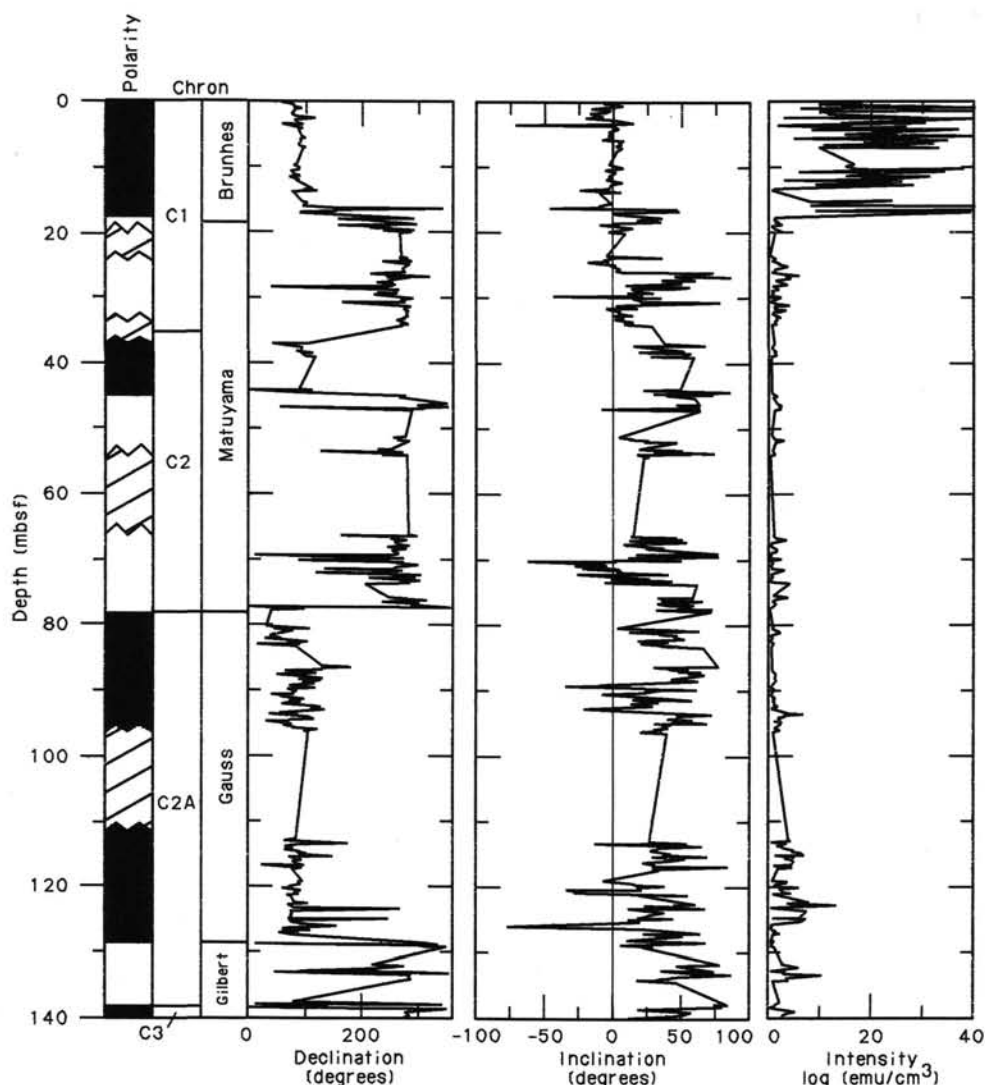


Figure 10. Data in Figure 7 replotted after exclusion of turbidite layers. Hatched zones indicate gaps in the record (polarity unknown).

ments are dominated by turbidites, which are characterized by high carbonate values of more than 75% CaCO_3 and low TOC values of less than 0.4% C_{org} (Fig. 13).

PHYSICAL PROPERTIES

Techniques used for our shipboard physical-property measurements at Site 666 are outlined in the "Introduction and Explanatory Notes" (this volume). Only one hole (666A) was cored at this site for which index properties and shear strength were measured throughout. These data are shown in Table 6 and in Figures 14 through 17. Profiles of the calcium carbonate content and grain density are shown in Figure 16. Hole 666A was logged continuously using the *P*-wave logger (PWL) and the GRAPE. A synthesis of the PWL data is given in Table 7. The PWL profile is shown in Figure 17. No data presented here were screened for bad data points.

The main feature of this site was the large number of reworked units that were present (turbidites and slumps; see "Lithostratigraphy and Sedimentology" section, this chapter). While this was somewhat detrimental to our primary objective of obtaining a complete pelagic sequence, it did present an interesting

P-wave log. Figure 18, which shows the log for Core 108-665A-2H, illustrates how distinctive these reworked units appear on the PWL profile.

SEISMIC STRATIGRAPHY

Hole 666A at Site 666 was drilled to a depth of 150.5 mbsf. The water-gun seismic profiler records obtained during our approach to Site 666 indicate two seismic units (Fig. 19) within this depth range:

Seismic unit 1, 0–0.05 s, is an upper unit with a false acoustic signal caused by the water guns. This unit should equate to the upper 38 m of sediment.

Seismic unit 2, 0.05–0.23 s, is a lower unit with a series of major reflectors, each composed of several smaller, more diffuse reflectors. This unit should equate to the interval of about 38 to 173 mbsf. This unit contains a particularly strong reflector at 0.125 s, equivalent to a depth of about 94 mbsf. The reflectivity of the acoustic layering is slightly stronger above this reflector than below the reflector, but no major change in acoustic character occurs across this level.

Table 2. Depth and age estimates of biostratigraphic and magnetostratigraphic indicators used to establish accumulation rates for Hole 666.

Datum	Depth (mbsf)	Age (Ma)
LO <i>Pseudoemiliana lacunosa</i>	9.1-10.6	0.47
Brunhes/Matuyama	18.4-18.4	0.73
LO <i>Calcidiscus macintyreii</i>	32.9-33.3	1.45
Matuyama/Olduvai	34.5-37.1	1.66
Olduvai/Matuyama	45.0-45.1	1.88
LO <i>Discoaster brouweri</i>	46.0-48.6	1.89
FO <i>D. triradiatus acme</i>	51.6-54.4	2.07
LO <i>Globorotalia miocenica</i>	46.0-55.5	2.20
LO <i>Discoaster pentaradiatus</i>	67.0-68.3	2.35
LO <i>D. surculus</i>	70.0-75.7	2.45
Matuyama/Gauss	77.5-80.6	2.47
LO <i>D. tamalis</i>	75.7-86.9	2.65
LO <i>Sphaeroidinellopsis seminulina</i>	93.0-103.0	3.00
LO <i>Pulleniatina</i> Gauss/Gilbert	126.3-128.5	3.40
LO <i>Sphenolithus abies</i>	123.1-128.3	3.45
LO <i>Reticulofenestra pseudoumbilica</i>	128.3-133.3	3.56
LO <i>Globigerina nepenthes</i>	144.7-150.5	3.90
FO <i>Globorotalia crassaformis</i>	144.7-150.5	4.20
FO/LO <i>Ceratolithus rugosus/C. acutus</i>	144.9-150.5	4.60
<i>C. acutus</i> present	150.5	5.00

Note: LO = last occurrence. FO = first occurrence.

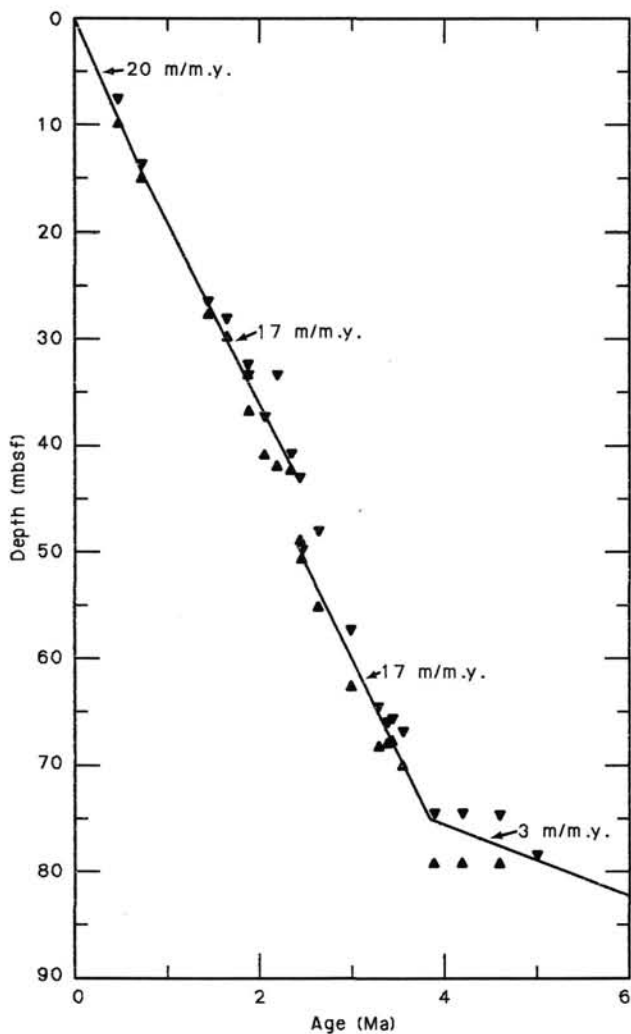


Figure 11. Age-depth curve for stratigraphic events in Hole 666A.

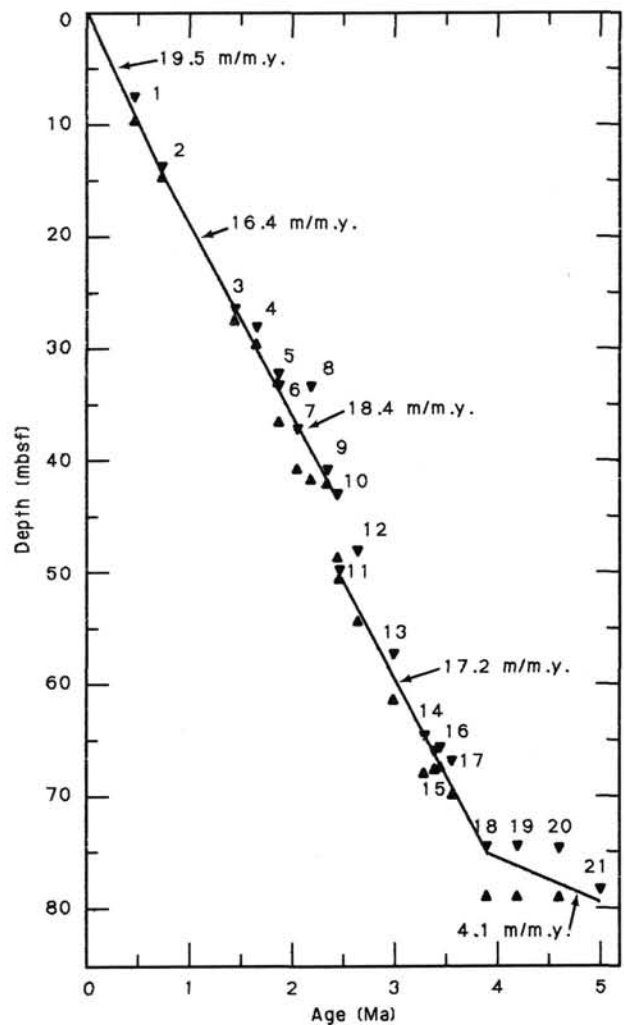


Figure 12. Graphic representation of sediment-accumulation rates for Hole 666A after removal of sediments identified as allochthonous.

Table 3. Depth and age estimates of biostratigraphic and magnetostratigraphic indicators used to establish accumulation rates for Hole 666 after correcting for slumps.

Datum	Depth (mbsf)	Age (Ma)
LO <i>Pseudoemiliana lacunosa</i>	7.9-9.4	0.47
Brunhes/Matuyama	14.0-14.5	0.73
LO <i>Calcidiscus macintyreii</i>	26.8-27.2	1.45
Matuyama/Olduvai	28.4-29.3	1.66
Olduvai/Matuyama	32.7-32.8	1.88
LO <i>Discoaster brouweri</i>	33.7-36.3	1.89
FO <i>D. triradiatus acme</i>	37.6-40.4	2.07
LO <i>Globorotalia miocenica</i>	33.7-41.4	2.20
LO <i>Discoaster pentaradiatus</i>	41.1-41.8	2.35
LO <i>D. surculus</i>	43.3-48.4	2.45
Matuyama/Gauss	50.2-50.2	2.47
LO <i>D. tamalis</i>	48.4-54.0	2.65
LO <i>Sphaeroidinellopsis seminulina</i>	57.7-62.1	3.00
LO <i>Pulleniatina</i> Gauss/Gilbert	64.9-67.7	3.30
LO <i>Sphenolithus abies</i>	66.3-67.4	3.40
LO <i>Sphenolithus abies</i>	66.0-67.2	3.45
LO <i>Reticulofenestra pseudoumbilica</i>	67.2-69.5	3.56
LO <i>Globigerina nepenthes</i>	74.8-78.7	3.90
FO <i>Globorotalia crassaformis</i>	74.8-78.7	4.20
FO/LO <i>Ceratolithus rugosus/C. acutus</i>	75.0-78.7	4.60
<i>C. acutus</i> present	78.7	5.00

Note: mbsf corrected for slumps.

Table 4. Results of inorganic-geochemical analyses conducted for Site 666.

Core/section	pH	Alkalinity (mmol/L)	Salinity (‰)	Chlorinity (mmol/L)	SO ₄ ²⁻ (mmol/L)	Mg ²⁺ (mmol/L)	Ca ²⁺ (mmol/L)
2-5	7.63	3.89	34.0	579	24.33	51.95	10.89
7-5	7.53	3.52	34.2	561	25.50	50.97	11.24
12-4	7.44	4.31	33.5	553	22.92	49.01	10.53

Table 5. Results of Rock-Eval pyrolysis, Site 666.

Sample (cm)	TOC (%)	HI	OI	C _{org}
1-1, 30	0.42	257	1869	M/T
1-2, 17	1.35	215	352	M/T
1-3, 96	0.76	141	991	M/T
1-5, 77	0.44	389	1225	M
2-1, 120	0.99	93	589	T
2-3, 120	0.27	411	3707	M
2-5, 120	0.24	367	2125	M
3-1, 125	0.33	64	1058	T
3-5, 120	0.18	245	2650	M/T
4-1, 120	0.25	200	2688	M/T
4-5, 120	0.26	231	962	M/T
5-1, 120	0.23	96	1509	T
5-5, 120	0.20	240	1115	M/T
6-1, 120	0.17	188	2412	M/T
6-5, 100	0.31	197	1136	M/T

M/T = mixed C_{org}; T = dominantly terrigenous; M = dominantly marine C_{org}; HI = hydrogen index; OI = oxygen index.

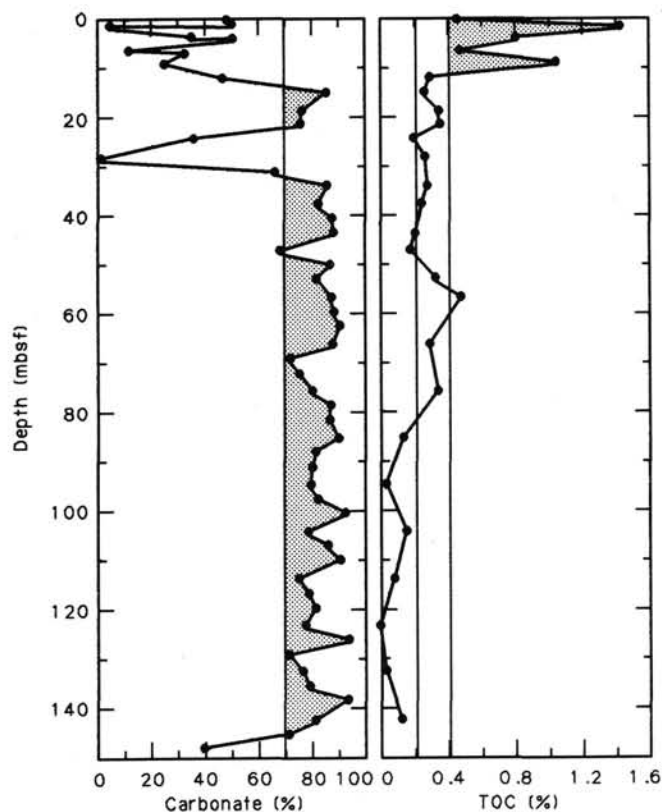


Figure 13. Carbonate and total-organic-carbon record for Hole 666A.

Table 6. Index-properties and vane-shear-strength data for Hole 666A.

Core/section	Interval (cm)	Depth (mbsf)	Grain density (g/cm ³)	Wet-water content (%)	Dry-water content (%)	Wet-bulk density (g/cm ³)	Dry-bulk density (g/cm ³)	Porosity (%)	Vane shear strength (kPa)
1-4	121	1.21	2.37	61.43	159.24	1.31	0.55	a---	6.60
1-2	121	2.71	2.54	61.98	163.01	1.32	0.54	80.45	5.80
1-3	121	4.21	2.49	61.01	156.47	1.32	0.56	74.51	8.62
1-4	121	5.71	2.66	69.83	220.81	1.26	0.44	85.45	11.40
1-5	121	7.21	2.30	68.00	212.50	1.24	0.44	---	11.00
2-1	121	---	2.35	65.97	193.84	1.26	0.48	---	16.00
2-2	111	10.61	2.60	56.93	132.17	1.38	0.64	---	28.00
2-3	121	12.21	2.54	59.08	144.39	1.35	0.60	79.53	16.00
2-4	121	13.71	2.61	52.99	112.70	1.43	0.71	74.46	0.00
2-5	11	14.11	2.62	56.04	127.46	1.39	0.65	76.80	0.00
2-5	71	14.71	2.60	54.20	118.34	1.41	0.69	75.32	0.00
2-5	121	15.21	2.65	52.90	112.30	1.44	0.73	74.54	0.00
2-6	111	16.61	2.37	63.61	174.83	1.29	0.52	83.51	43.00
3-1	126	19.76	2.52	57.04	132.80	1.37	0.63	76.86	22.00
3-2	126	20.26	2.56	54.10	117.88	1.41	0.68	74.95	29.00
3-3	126	21.76	2.63	52.10	108.76	1.44	0.73	73.91	25.00
3-4	126	23.26	2.55	56.70	130.94	1.38	0.65	76.86	3.00
3-5	111	24.61	2.49	52.62	141.67	1.35	0.60	77.82	26.00
3-6	121	26.21	2.58	53.78	103.18	1.45	0.76	72.53	15.00
4-1	121	28.21	2.74	53.44	110.25	1.45	0.72	74.97	25.00
4-2	171	29.71	2.72	47.07	88.94	1.52	0.84	70.91	23.00
4-3	121	31.21	2.59	---	90.06	1.50	0.82	---	27.00
4-4	121	32.71	2.66	47.51	50.51	1.51	0.83	70.47	34.00
4-5	121	34.21	2.59	52.80	111.88	1.43	0.72	74.20	22.00
5-1	121	37.71	2.62	52.04	100.16	1.47	0.77	77.19	20.00
5-2	121	39.21	2.62	---	98.75	1.47	0.78	71.92	26.00
5-3	121	40.71	2.58	56.29	128.77	1.39	0.65	76.73	0.00
5-4	121	42.21	2.60	50.89	103.63	1.45	0.76	---	0.00
5-5	121	---	2.64	45.39	97.59	1.48	---	71.84	0.00
5-6	121	45.21	2.64	47.13	99.13	1.51	0.84	65.99	23.00
6-1	121	---	2.80	45.42	83.20	1.56	0.88	---	27.00
6-2	121	48.71	2.62	44.36	79.74	1.54	0.90	---	28.00
6-3	121	50.21	2.64	51.35	105.56	1.45	0.75	73.42	0.00

Table 6 (continued).

Core/ section	Interval (cm)	Depth (mbsf)	Grain density (g/cm ³)	Wet-water content (%)	Dry-water content (%)	Wet-bulk density (g/cm ³)	Dry-bulk density (g/cm ³)	Porosity (%)	Vane shear strength (kPa)
6-4	121	51.71	2.72	47.29	89.71	1.52	0.85	70.74	34.00
6-5	101	53.01	2.66	44.26	79.39	1.55	0.91	67.60	30.00
6-6	111	54.61	2.65	41.93	72.21	1.59	0.93	65.43	25.00
7-1	121	56.71	2.25	52.89	112.27	1.37	0.69	71.48	0.00
7-2	121	58.21	2.61	49.37	97.51	1.47	0.77	71.57	0.00
7-3	121	59.71	2.65	47.03	88.78	1.51	0.83	69.94	0.00
7-4	121	61.21	2.63	50.72	102.90	1.46	0.75	---	0.00
7-5	121	62.71	2.89	---	99.60	1.51	0.79	71.01	0.00
7-6	121	64.21	2.58	48.79	95.26	1.48	0.81	---	0.00
8-1	121	66.21	2.51	---	91.26	1.48	0.82	---	0.00
8-2	121	67.71	2.65	---	64.97	1.63	1.01	63.00	27.00
8-3	121	---	2.62	40.82	68.98	1.60	---	64.14	34.00
8-4	121	70.71	2.64	41.42	70.71	1.59	0.97	---	35.00
8-5	121	72.21	2.61	42.36	73.51	1.57	0.96	---	35.00
8-6	121	73.71	2.67	45.33	82.93	1.54	0.88	---	20.00
9-1	121	73.71	2.61	---	80.97	1.54	0.84	---	20.00
9-2	121	---	2.64	41.92	72.18	1.59	0.96	65.36	34.00
9-3	121	78.71	2.61	52.92	112.40	1.43	0.71	---	0.00
9-4	121	80.21	2.66	53.99	117.32	1.42	0.70	---	0.00
9-5	111	81.61	2.63	45.18	82.41	1.53	0.88	---	29.00
9-6	121	83.21	2.63	45.87	69.13	1.60	0.99	64.25	27.00
10-1	121	93.21	2.60	---	118.80	1.41	---	---	0.00
10-2	121	---	2.64	42.24	73.13	1.58	---	65.63	---
10-3	121	55.21	2.62	43.77	74.75	1.57	0.95	---	32.00
10-4	101	---	2.64	51.51	106.21	1.45	0.74	---	0.00
10-4	121	---	2.66	42.30	76.37	1.57	0.73	66.75	30.00
10-5	121	---	2.80	44.80	81.17	1.57	0.90	65.20	24.00
10-6	121	---	2.73	41.58	71.10	1.61	0.98	65.79	---
11-1	121	54.71	2.62	42.54	74.03	1.57	0.93	65.69	23.00
11-2	121	---	2.67	---	65.18	1.63	1.03	63.24	45.00
11-3	121	---	2.64	---	63.17	1.64	1.06	62.27	27.00
11-4	121	---	2.70	46.22	85.95	1.53	0.87	---	0.00
11-5	101	100.51	2.63	45.09	82.12	1.54	0.88	69.08	0.00
11-6	121	102.21	2.51	40.55	68.21	1.58	---	67.95	28.00
12-1	121	104.21	2.60	37.19	59.21	1.65	1.08	60.31	29.00
12-2	121	105.71	2.58	47.89	91.89	1.49	0.85	---	0.00
12-3	121	---	2.59	43.38	76.62	1.55	0.92	---	---
12-4	121	106.71	2.70	39.19	61.79	1.66	1.07	62.26	25.00
12-5	101	110.01	2.62	47.23	89.51	1.50	0.82	---	0.00
12-6	101	111.51	2.54	43.94	84.97	1.51	0.86	---	62.00
13-1	121	113.71	2.45	37.64	60.37	1.60	1.04	---	55.00
13-2	121	115.21	---	---	57.71	1.68	1.11	---	40.00
13-3	121	---	2.61	---	58.44	1.66	---	60.14	28.00
13-4	121	---	2.59	---	91.72	1.49	0.81	---	0.00
13-5	121	119.71	2.64	39.21	64.50	1.63	1.03	---	28.00
13-6	121	---	2.58	38.94	63.77	1.62	1.04	61.50	34.00
14-1	121	123.21	2.60	37.91	61.05	1.64	1.07	61.03	27.00
14-2	121	124.71	2.71	38.19	61.79	1.66	1.07	67.33	29.00
14-3	121	126.21	2.61	47.35	89.93	1.50	0.83	---	0.00
14-4	121	---	2.58	38.69	63.11	1.62	1.04	61.65	33.03
14-5	121	---	2.60	37.82	60.83	1.64	1.07	---	34.00
14-6	121	130.71	2.58	44.36	78.72	1.54	0.90	---	19.00
15-1	101	---	2.61	38.36	62.23	1.63	1.06	61.64	37.00
15-2	121	134.21	2.67	40.03	66.75	1.62	1.01	---	21.00
15-3	121	135.71	2.63	36.49	57.46	1.67	1.10	57.68	29.00
15-4	121	137.21	2.60	---	87.05	1.51	0.84	---	0.00
15-5	101	138.51	2.61	---	90.63	1.50	0.82	---	0.00
15-6	101	140.01	2.64	37.81	60.80	1.65	1.07	---	32.00
16-1	---	142.41	2.67	36.84	58.32	1.67	1.10	60.59	50.00
16-2	31	142.81	2.69	35.75	55.64	1.70	1.13	---	---
16-3	121	145.21	2.63	36.50	57.47	1.67	1.10	---	72.00
16-4	6	145.56	2.79	36.52	57.54	1.71	1.13	61.29	59.00
16-5	121	149.21	2.68	35.10	54.08	1.71	1.15	---	90.00
16-6	141	149.91	2.65	35.00	53.85	1.70	1.16	---	68.00

^a No data available.

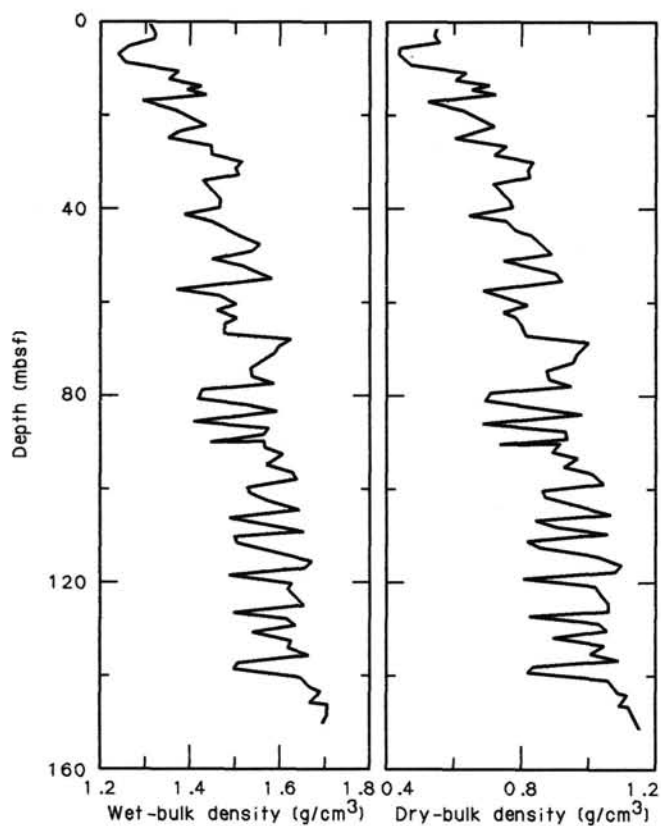


Figure 14. Wet- and dry-bulk-density profiles for Hole 666A.

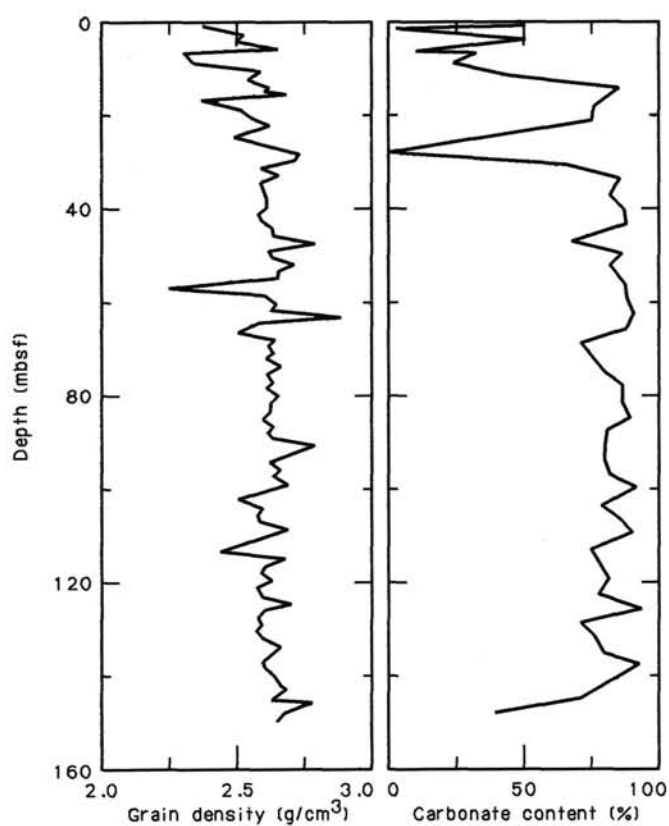


Figure 16. Grain-density and calcium carbonate profiles for Hole 666A.

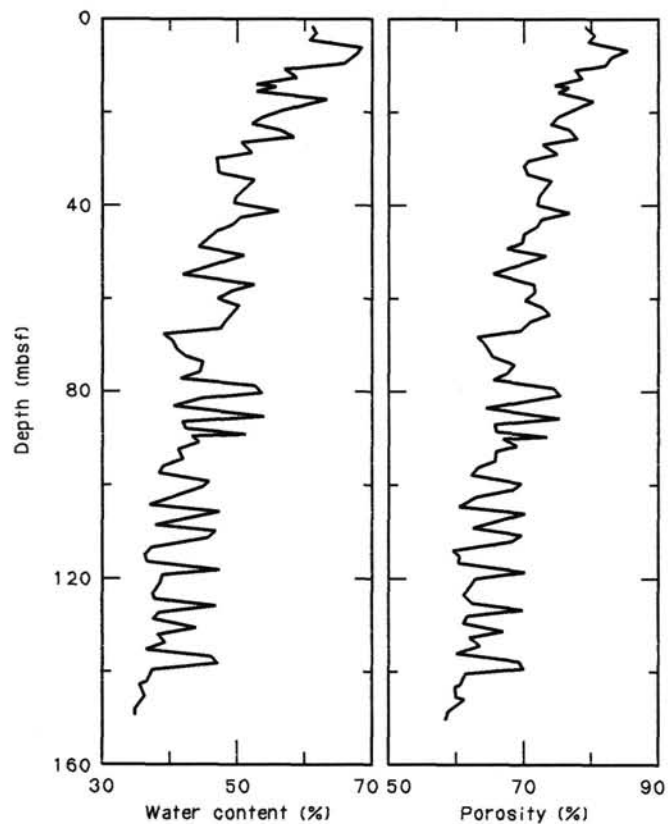


Figure 15. Water-content and porosity profiles for Hole 666A.

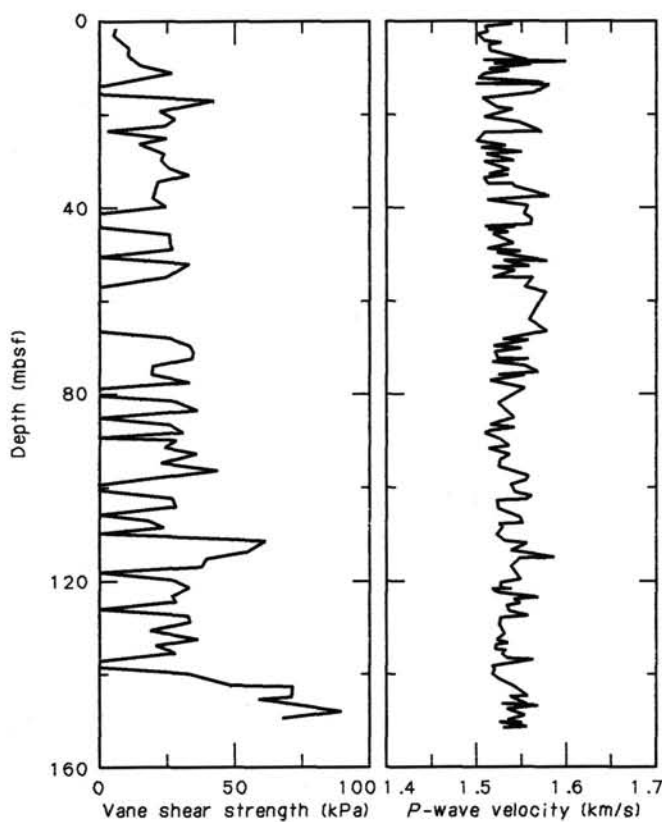


Figure 17. Vane-shear-strength and *P*-wave-velocity profiles for Hole 666A.

Table 7. Synthesis of P-wave logger velocity data for Hole 666A.

Depth (m)	Velocity (km/s)	Depth (m)	Velocity (km/s)
0.50	1.542	76.70	1.518
1.00	1.510	78.50	1.556
2.00	1.515	79.50	1.545
2.70	1.502	81.50	1.526
4.00	1.511	83.20	1.538
4.70	1.530	84.50	1.545
5.00	1.516	86.00	1.518
6.00	1.517	86.50	1.546
6.50	1.520	87.00	1.521
8.00	1.559	88.00	1.511
8.20	1.508	89.50	1.530
8.60	1.602	90.90	1.540
9.00	1.520	91.20	1.517
9.30	1.562	92.50	1.542
10.00	1.515	94.00	1.528
10.50	1.539	95.50	1.528
11.00	1.511	97.20	1.560
12.00	1.502	98.10	1.557
13.00	1.575	98.90	1.540
13.20	1.500	100.50	1.545
13.60	1.583	101.10	1.563
15.00	1.565	102.00	1.557
16.00	1.508	102.10	1.528
18.10	1.528	104.00	1.528
18.80	1.543	105.00	1.539
20.00	1.510	106.00	1.551
21.30	1.550	107.10	1.555
23.50	1.575	107.20	1.528
23.70	1.510	108.00	1.532
25.50	1.501	109.50	1.525
26.40	1.536	111.00	1.535
26.70	1.506	111.40	1.560
27.80	1.553	113.00	1.540
28.20	1.511	114.20	1.598
29.00	1.525	114.50	1.550
29.70	1.545	116.50	1.540
29.80	1.510	117.50	1.545
31.00	1.520	118.50	1.550
31.90	1.540	119.00	1.552
32.30	1.514	120.00	1.530
32.80	1.540	121.00	1.531
33.30	1.510	121.10	1.542
34.40	1.514	121.20	1.520
34.70	1.542	122.00	1.529
35.40	1.546	122.50	1.560
37.20	1.583	123.00	1.571
37.50	1.540	123.50	1.544
38.00	1.514	123.90	1.551
39.30	1.560	124.50	1.537
40.90	1.553	126.00	1.540
41.90	1.563	126.90	1.560
43.40	1.562	127.50	1.530
43.60	1.510	129.00	1.528
43.80	1.546	131.00	1.535
43.90	1.513	132.50	1.525
44.70	1.540	132.90	1.540
44.90	1.519	133.30	1.524
47.00	1.545	134.40	1.523
48.30	1.515	134.60	1.538
49.30	1.552	135.50	1.530
49.40	1.524	136.50	1.537
50.90	1.580	136.60	1.565
51.00	1.532	137.50	1.540
52.10	1.560	138.00	1.520
52.20	1.520	138.50	1.526
53.10	1.546	139.50	1.521
54.50	1.520	141.00	1.530
54.90	1.565	142.00	1.545
56.70	1.555	143.00	1.551
58.00	1.578	143.90	1.560
60.30	1.570	144.10	1.539
63.30	1.560	145.00	1.553

Table 7 (continued).

Depth (m)	Velocity (km/s)	Depth (m)	Velocity (km/s)
66.00	1.580	145.70	1.559
67.00	1.541	145.90	1.530
67.50	1.531	146.40	1.570
68.00	1.560	146.40	1.570
69.00	1.520	146.50	1.535
69.60	1.553	147.00	1.550
70.30	1.521	148.00	1.557
72.00	1.527	149.00	1.536
72.40	1.560	149.40	1.554
72.60	1.521	149.60	1.527
73.70	1.554	150.00	1.551
75.10	1.572	150.50	1.580
75.40	1.527	150.60	1.531
75.70	1.558		

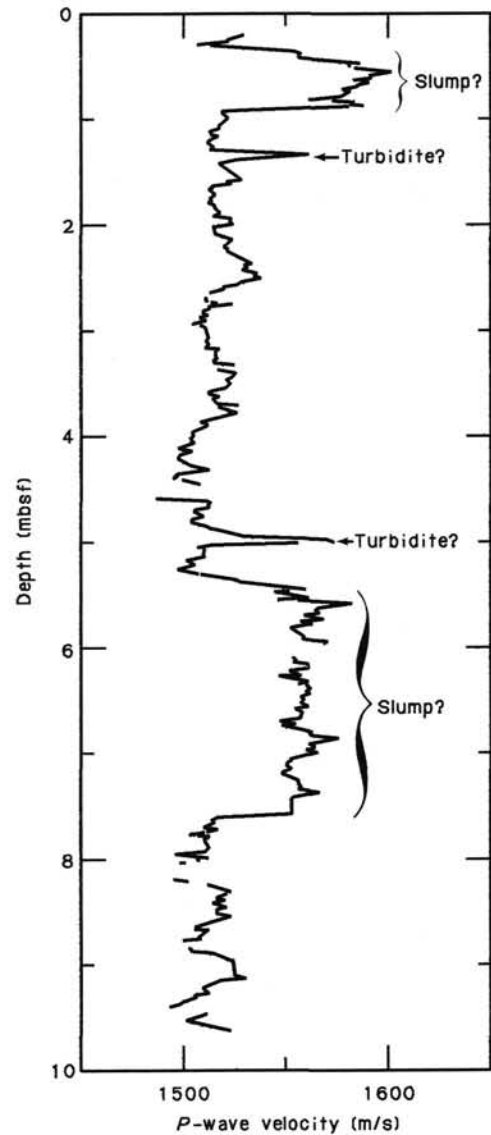


Figure 18. Detailed P-wave-logger profile for Core 108-666A-2H, showing the distinctive character of what are probably slumps and turbidites.

We used a mean two-way traveltime sound velocity of 760 m/s for the entire sediment section at Site 666 (see "Physical Properties" section, this chapter) to evaluate possible correlations of the seismic units with lithologic units (Fig. 19). Seismic unit 1 is an artifact. Seismic unit 2 corresponds approximately to lithologic Unit I, the sequence of layered Pliocene and Pleistocene nannofossil and clay-bearing oozes interrupted by numerous turbidites composed of redistributed pelagic (foraminifer-rich) sediments. Seismic unit 2, however, also includes the top of lithologic Unit II, the lower Pliocene, clayey nannofossil ooze that probably grades downward into the red-clay facies observed at Site 665 (see "Lithostratigraphy and Sedimentology" section, this chapter). Thus, no obvious correlation exists between seismic and lithologic units.

We also note that the acoustic character of the water-gun records obtained during the approach to Site 666 (which contained numerous turbidites) was not fundamentally different from that obtained on the approach to Site 665 (which contained almost no turbidites). This suggests that in this region, severe limitations exist for using conventional seismic records to infer lithologic characteristics.

REFERENCES

- Gieskes, J. M., and Peretsman, G., 1986. Water chemistry procedures aboard the *JOIDES Resolution*. ODP Technical Report No. 5.
 Tissot, B. P., and Welte, D. H., 1984. *Petroleum Formation and Occurrence*: Berlin-Heidelberg (Springer-Verlag).

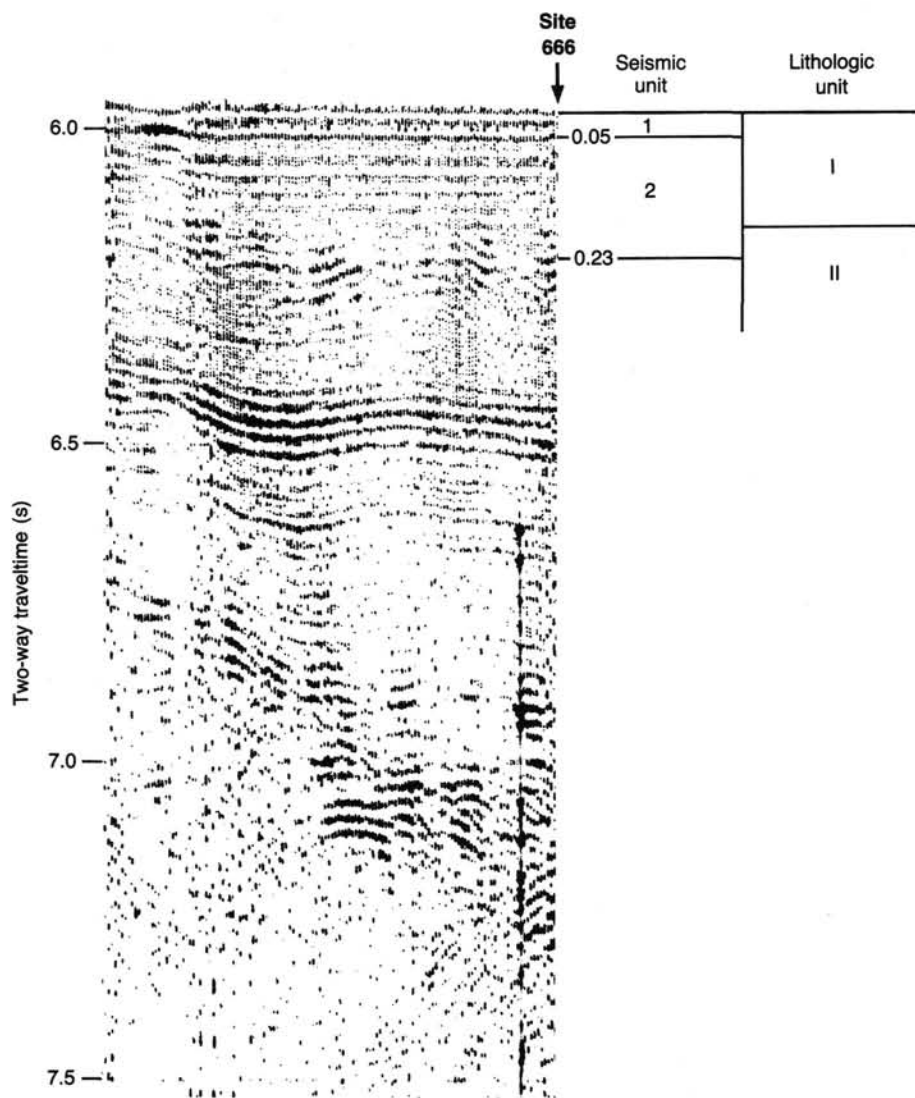
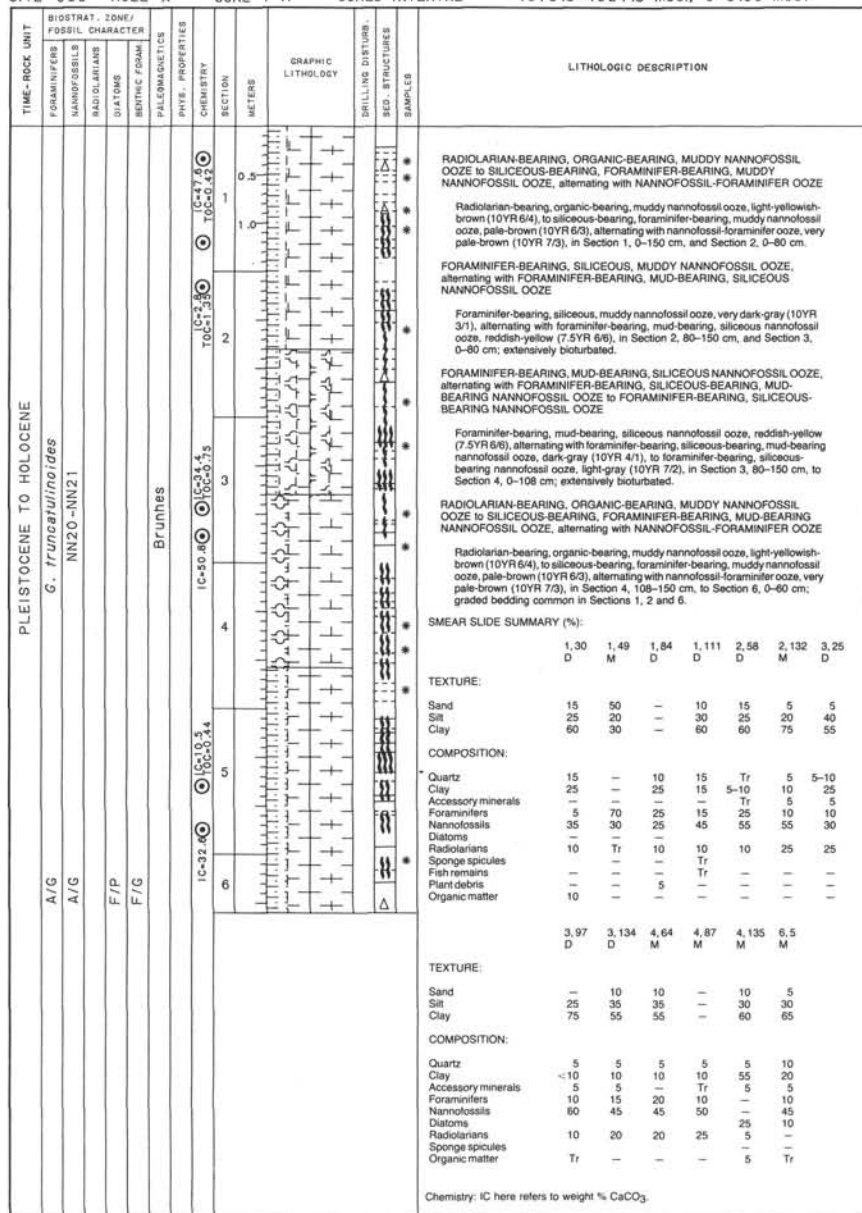
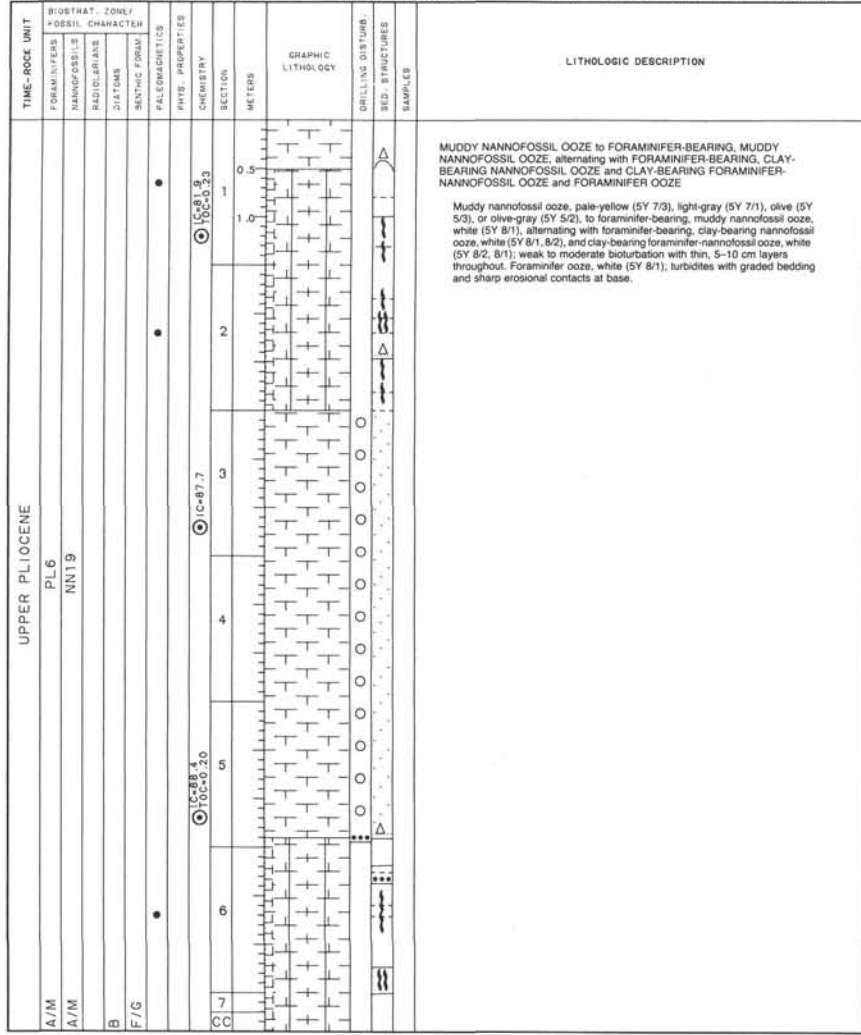


Figure 19. Comparison of Site 666 seismic units with lithologic units.

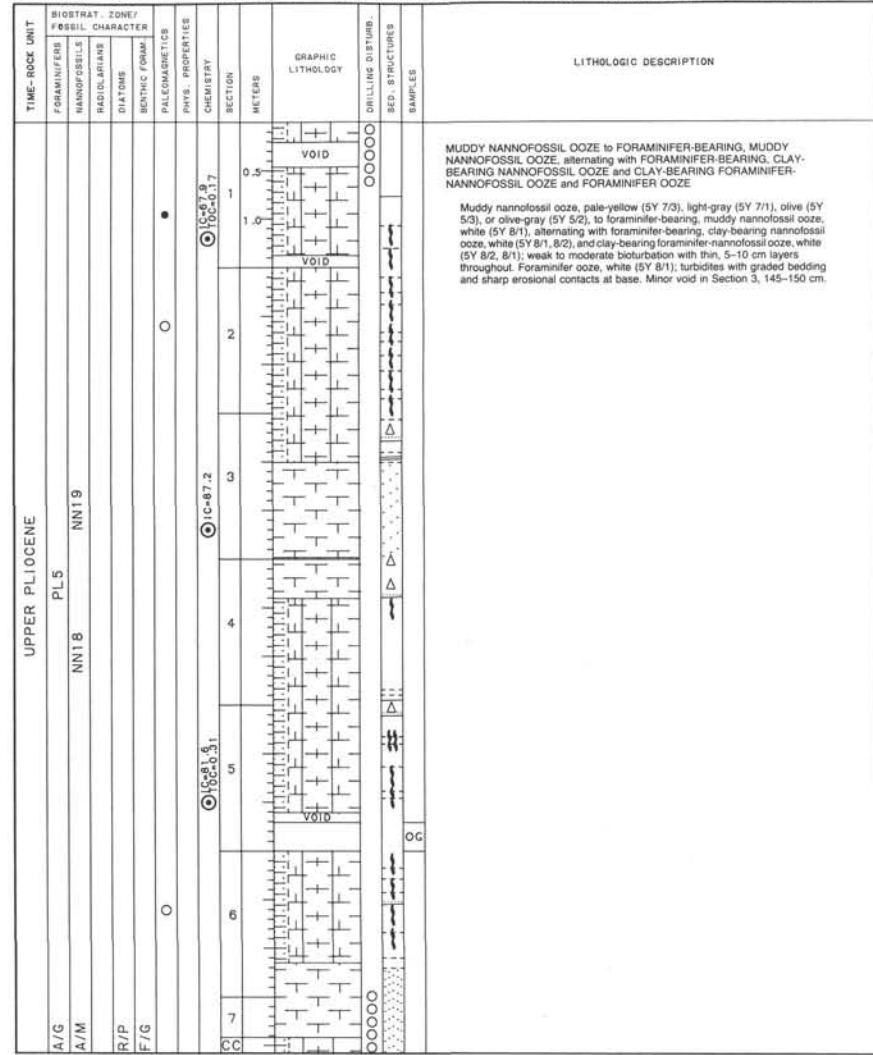
SITE 666 HOLE A CORE 1 H CORED INTERVAL 4516.8-4524.8 mbsl; 0-8.00 mbsf



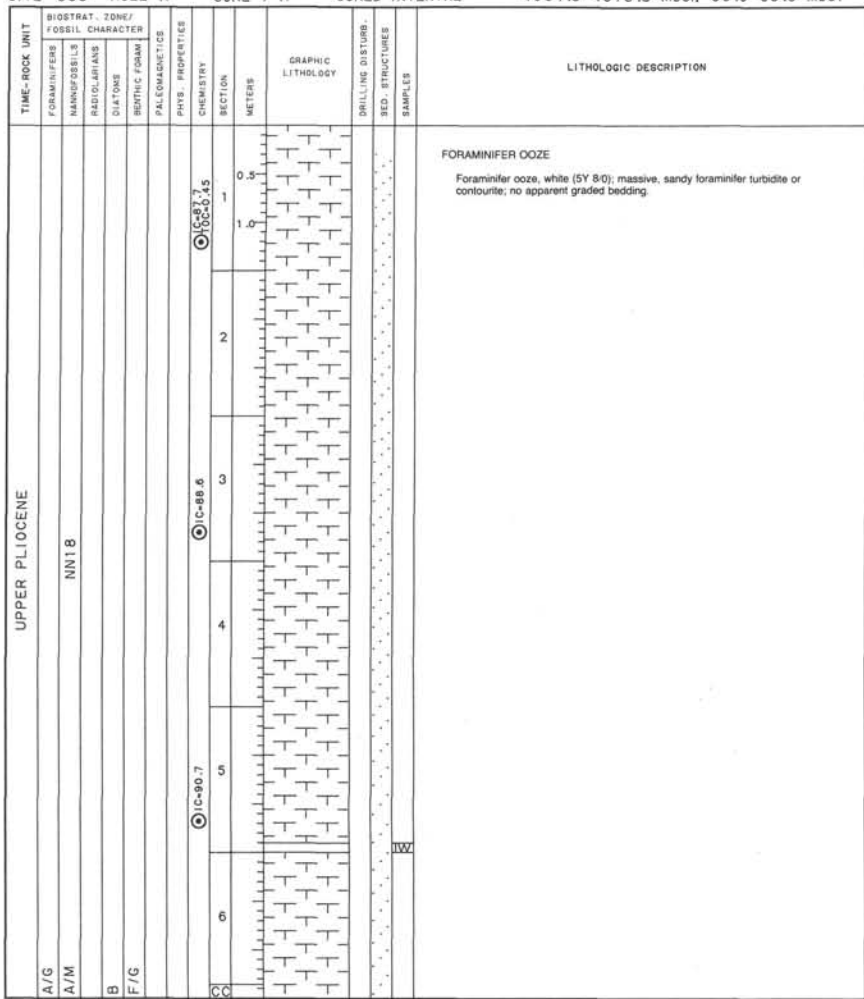
SITE 666 HOLE A CORE 5 H CORED INTERVAL 4545.3-4554.8 mbsl; 36.5-46.0 mbsf



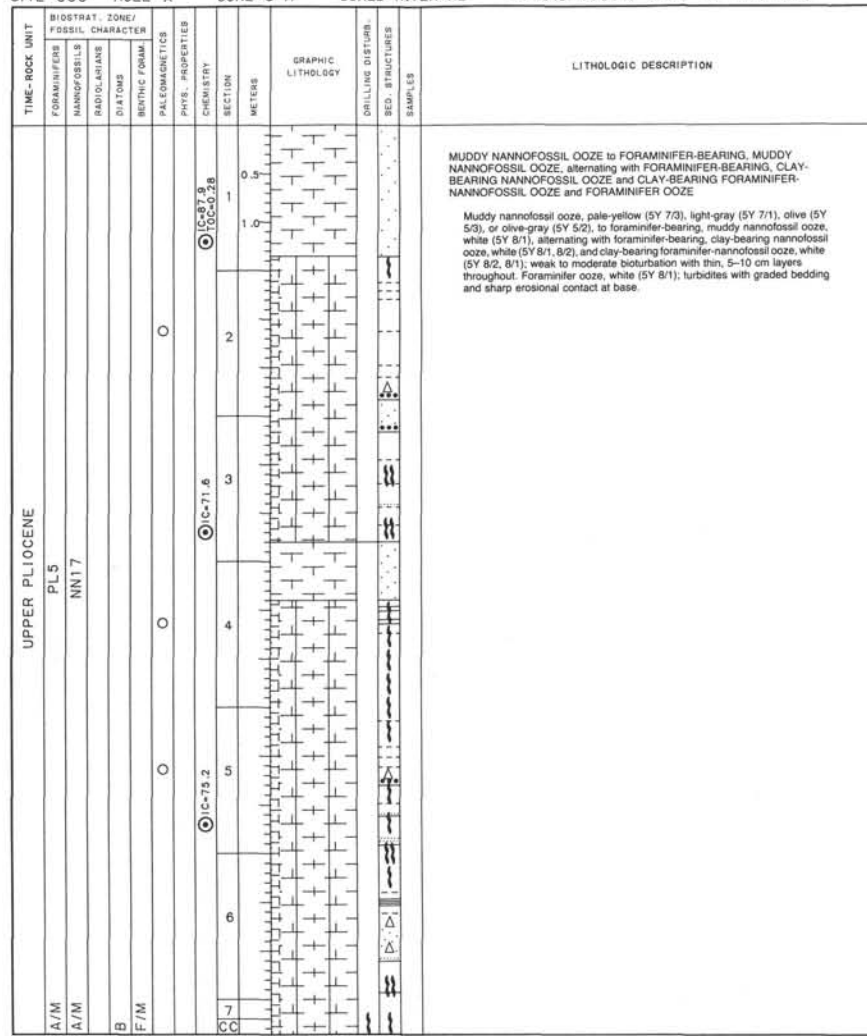
SITE 666 HOLE A CORE 6 H CORED INTERVAL 4554.8-4564.3 mbsl; 46.0-56.5 mbsf



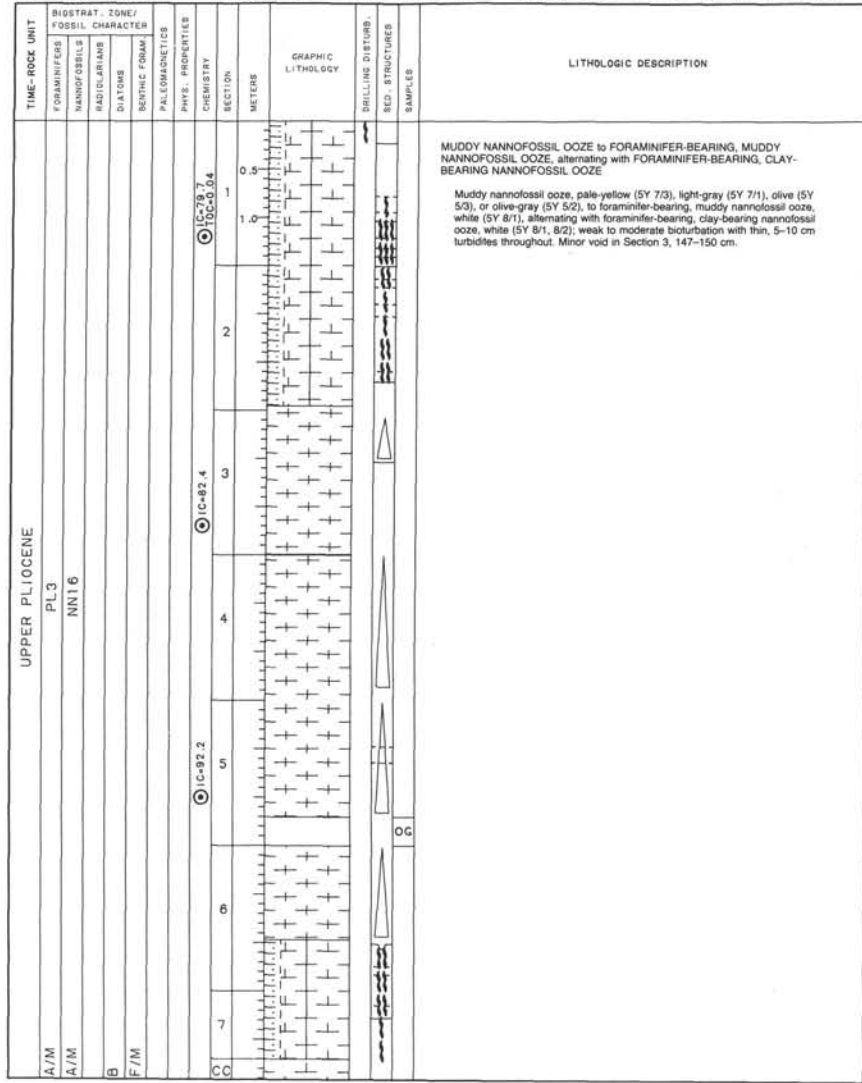
SITE 666 HOLE A CORE 7 H CORED INTERVAL 4564.3-4573.8 mbsl; 55.5-65.0 mbsf



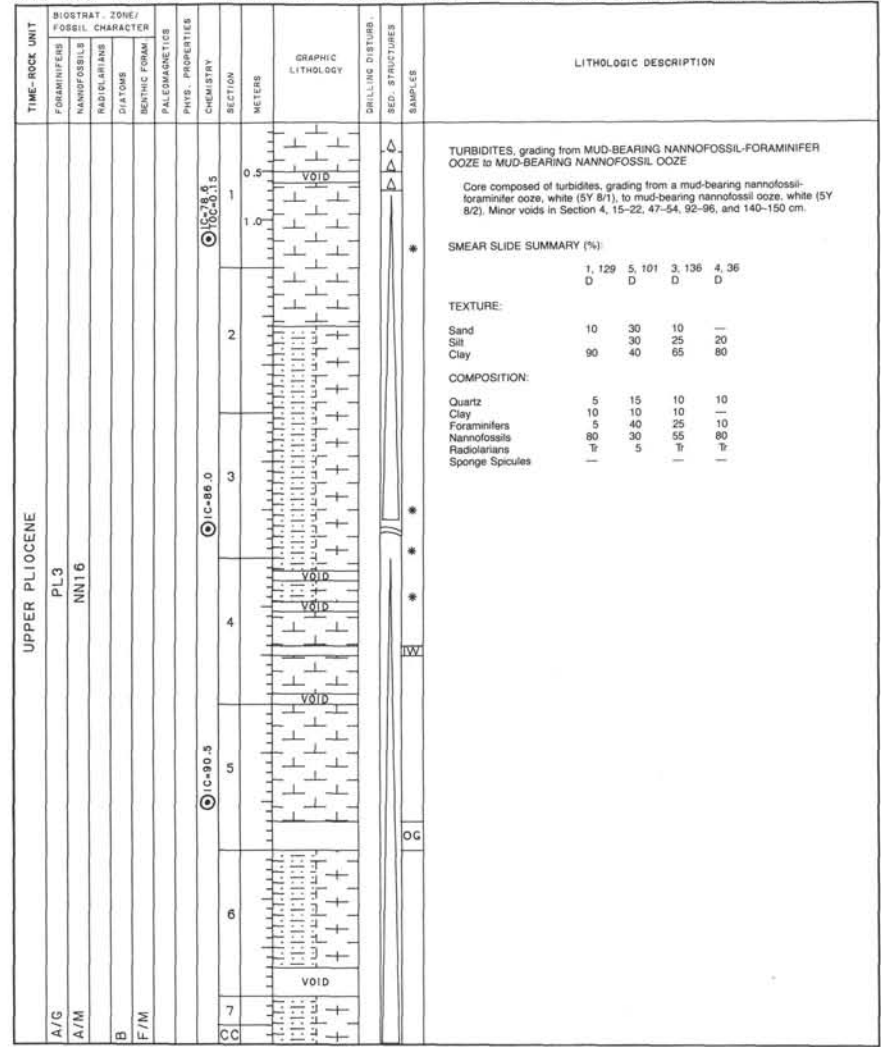
SITE 666 HOLE A CORE 8 H CORED INTERVAL 4573.8-4583.3 mbsl; 65-74.5 mbsf



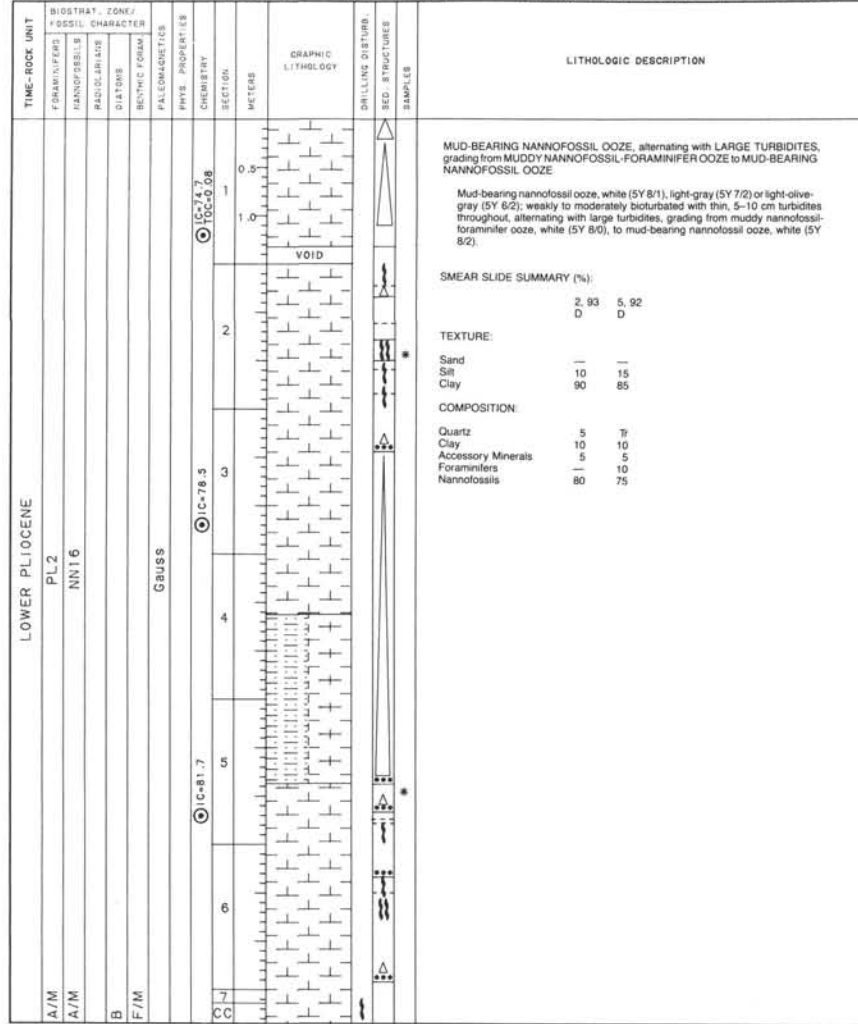
SITE 666 HOLE A CORE 11 H CORED INTERVAL 4602.3-4611.8 mbsl; 93.5-103.0 mbsf



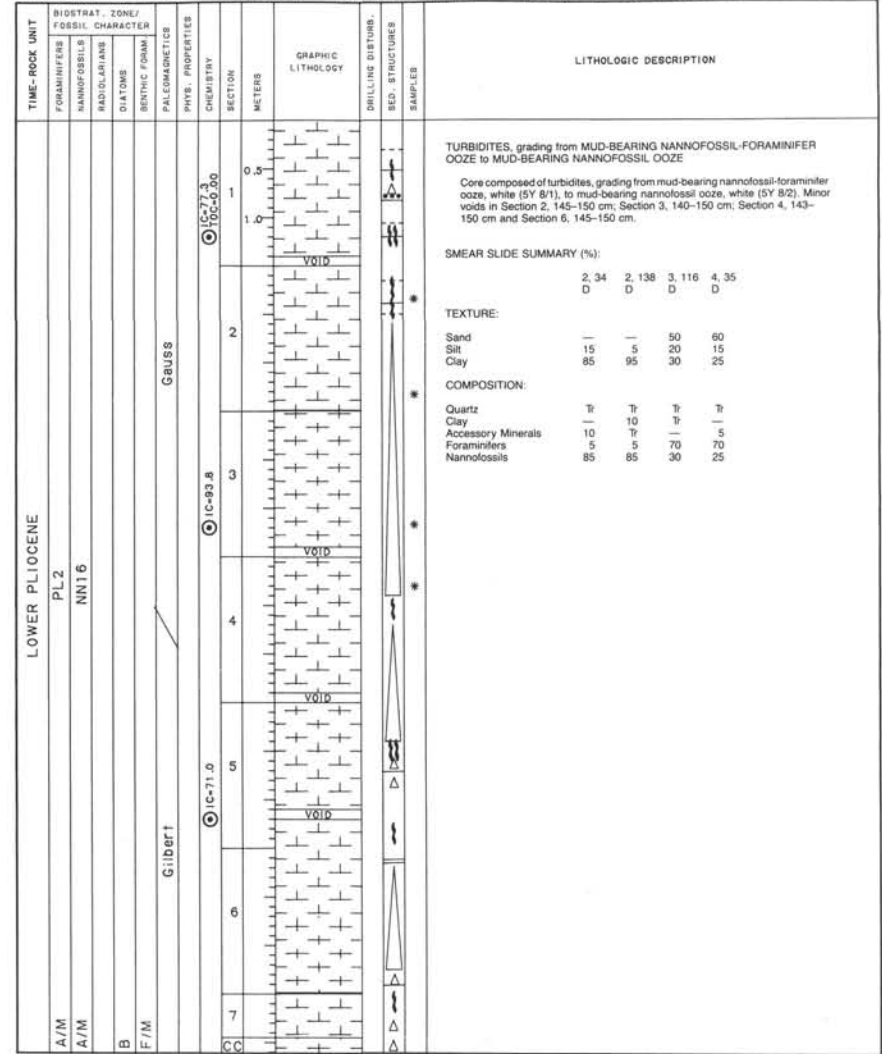
SITE 666 HOLE A CORE 12 H CORED INTERVAL 4611.8-4621.3 mbsl; 103-112.5 mbsf



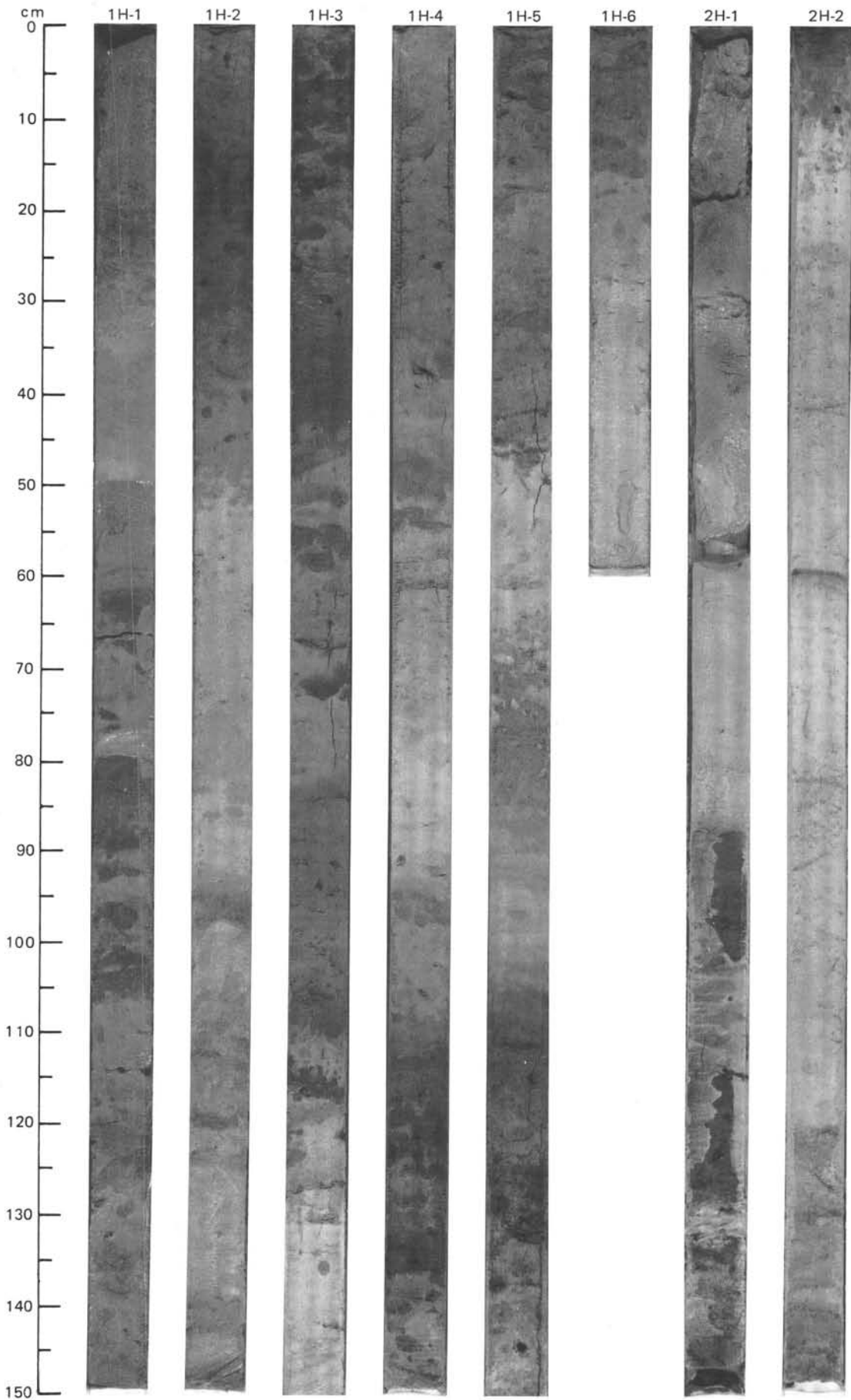
SITE 666 HOLE A CORE 13 H CORED INTERVAL 4621.3-4630.8 mbsf; 112.5-122 mbsf

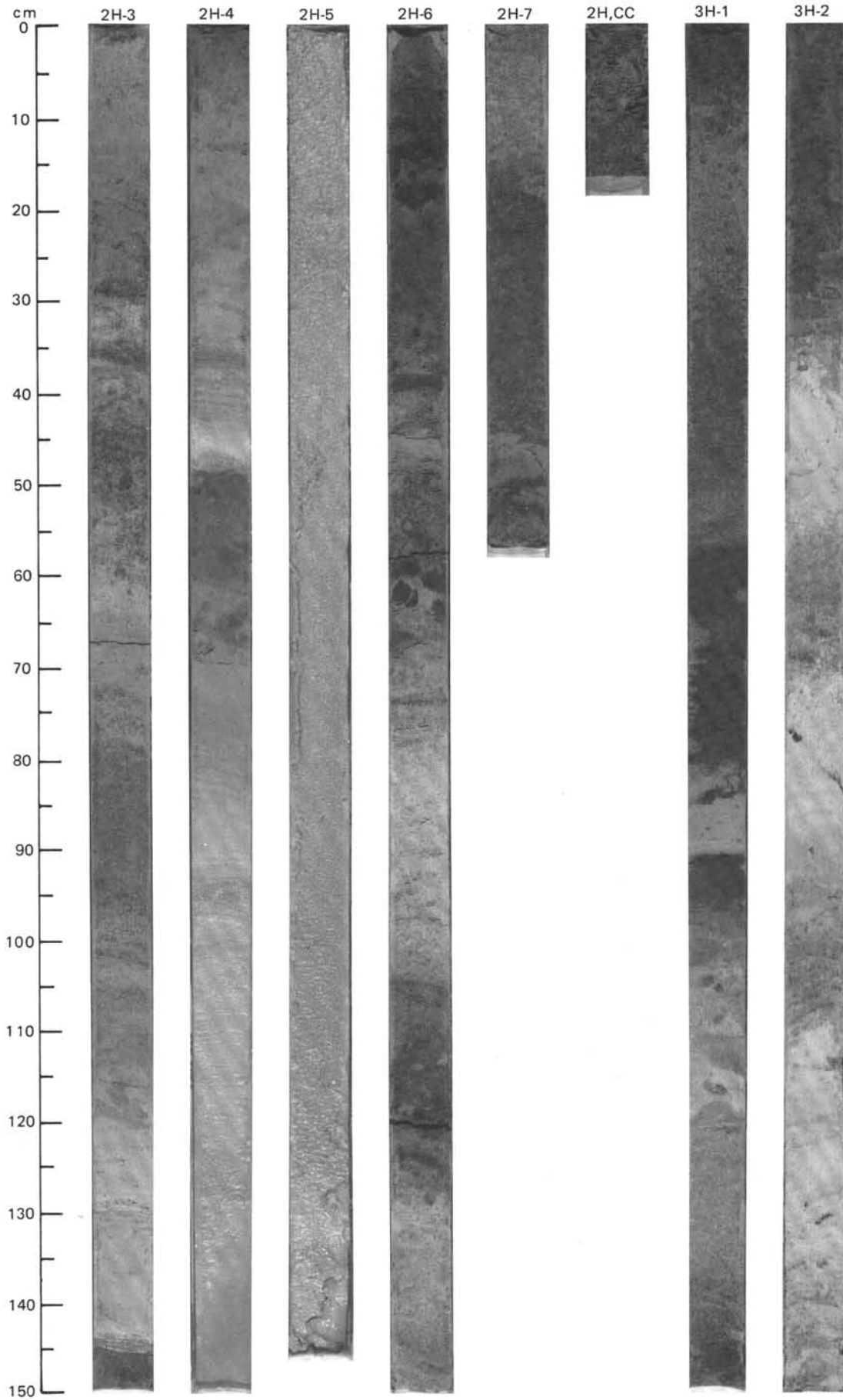


SITE 666 HOLE A CORE 14 H CORED INTERVAL 4630.8-4640.3 mbsf; 122-131.5 mbsf

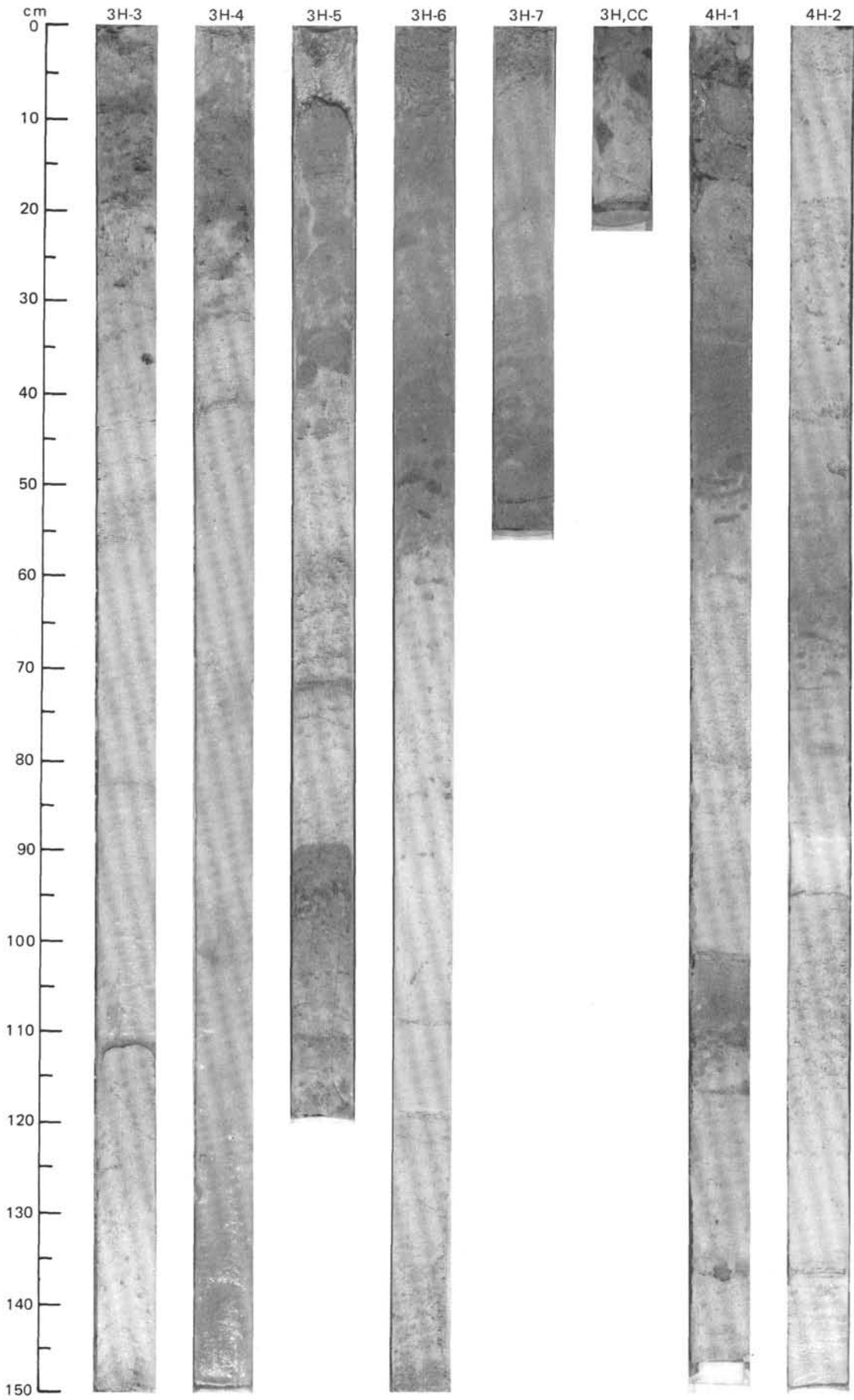


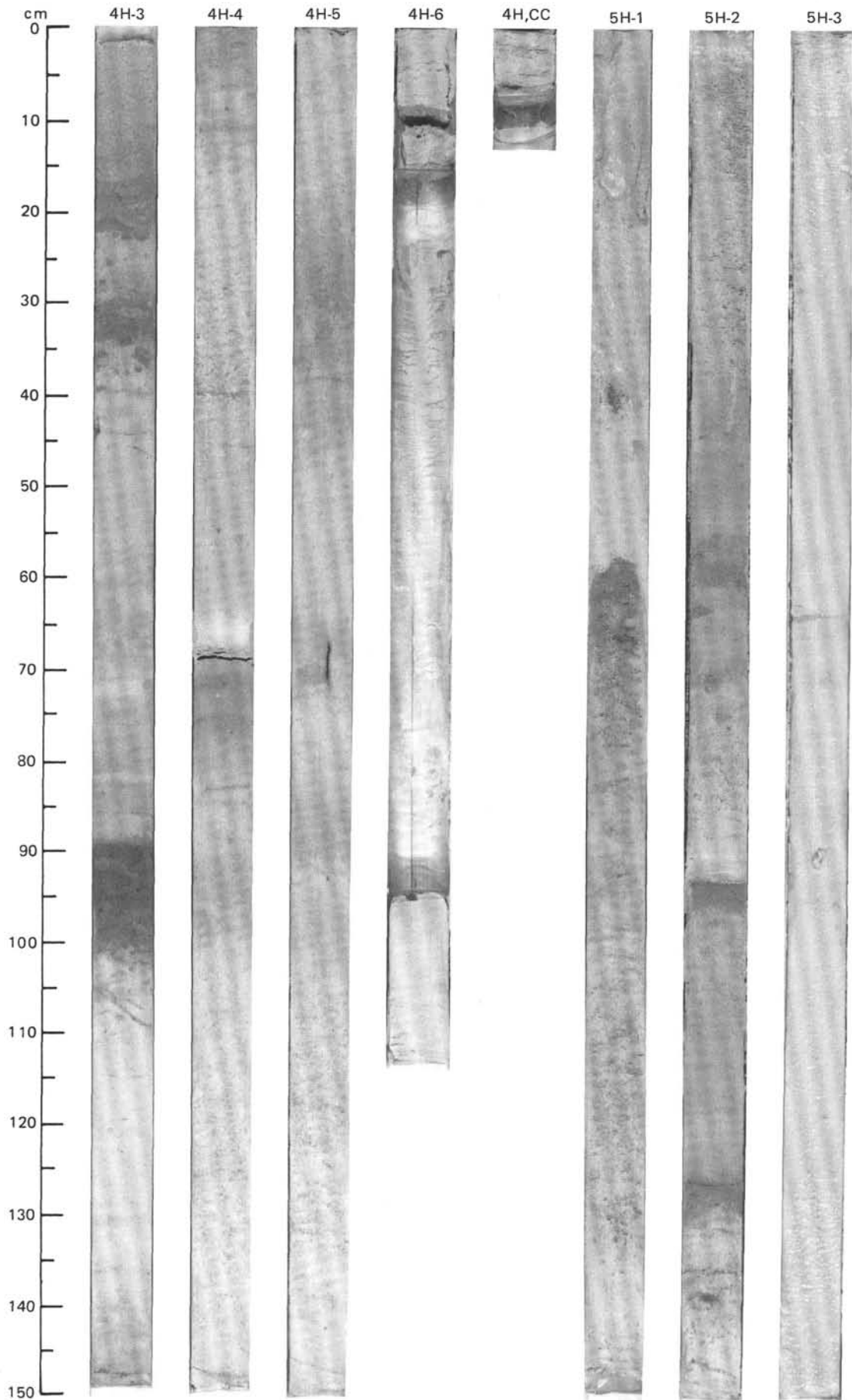
SITE 666 (HOLE A)



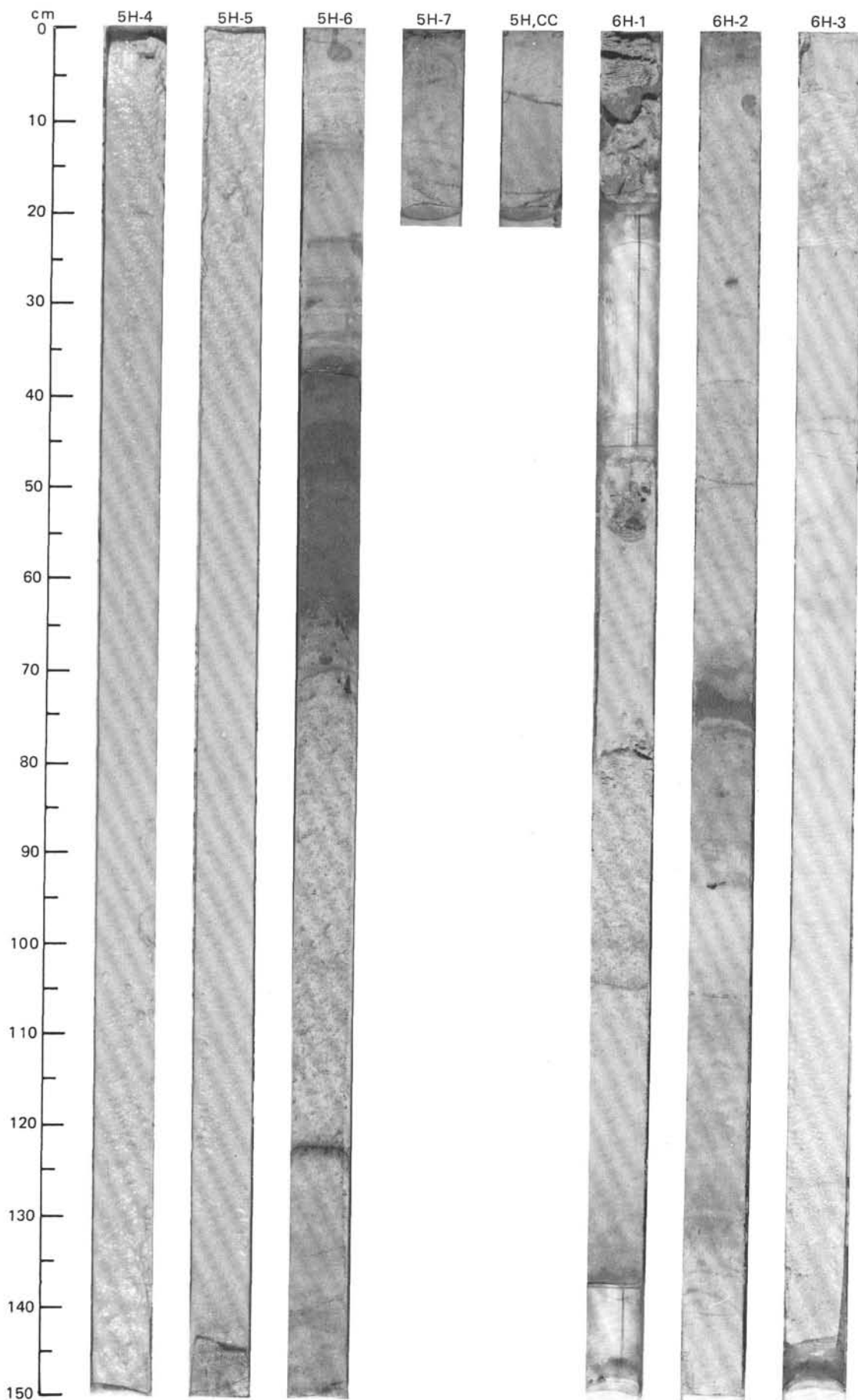


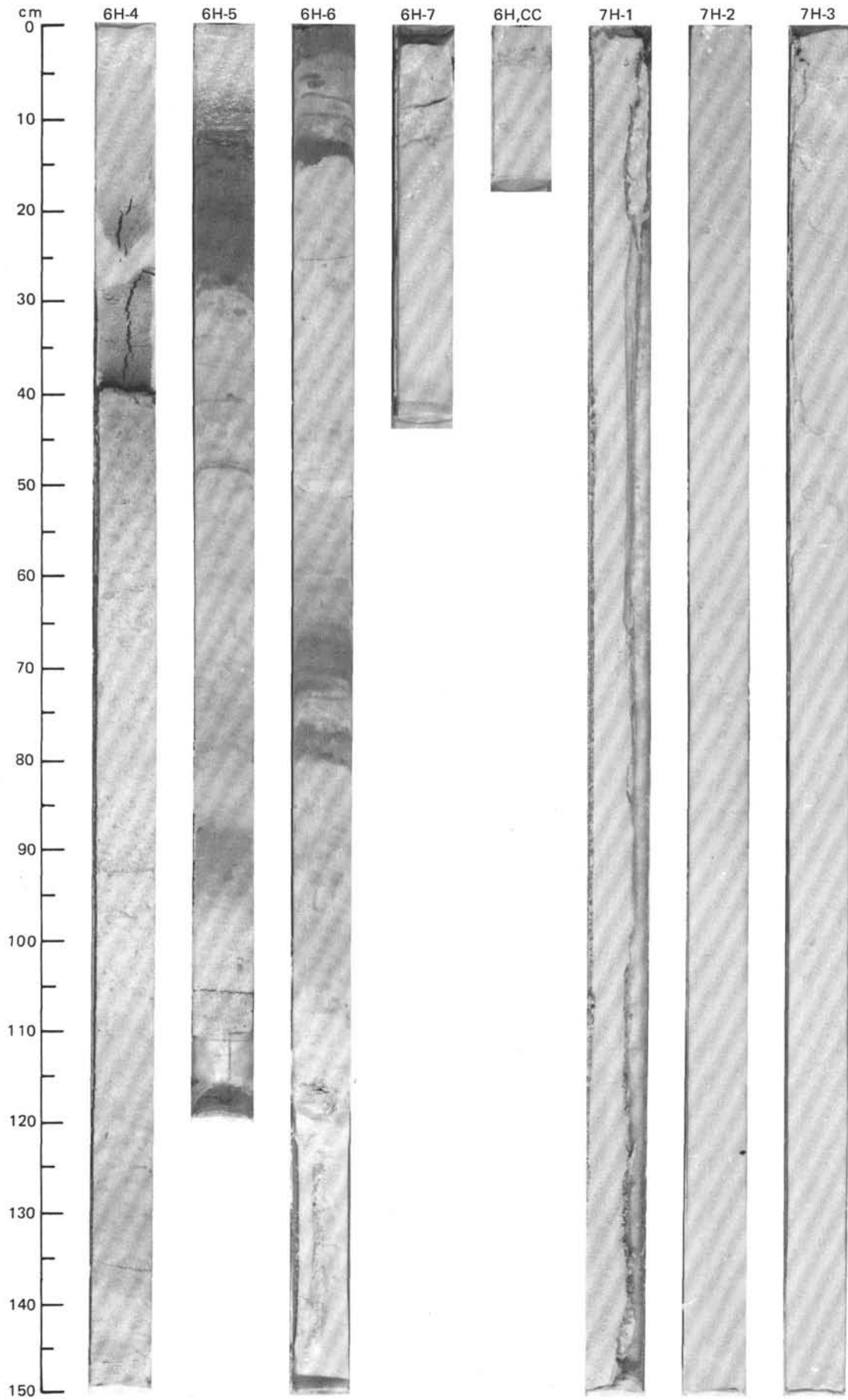
SITE 666 (HOLE A)



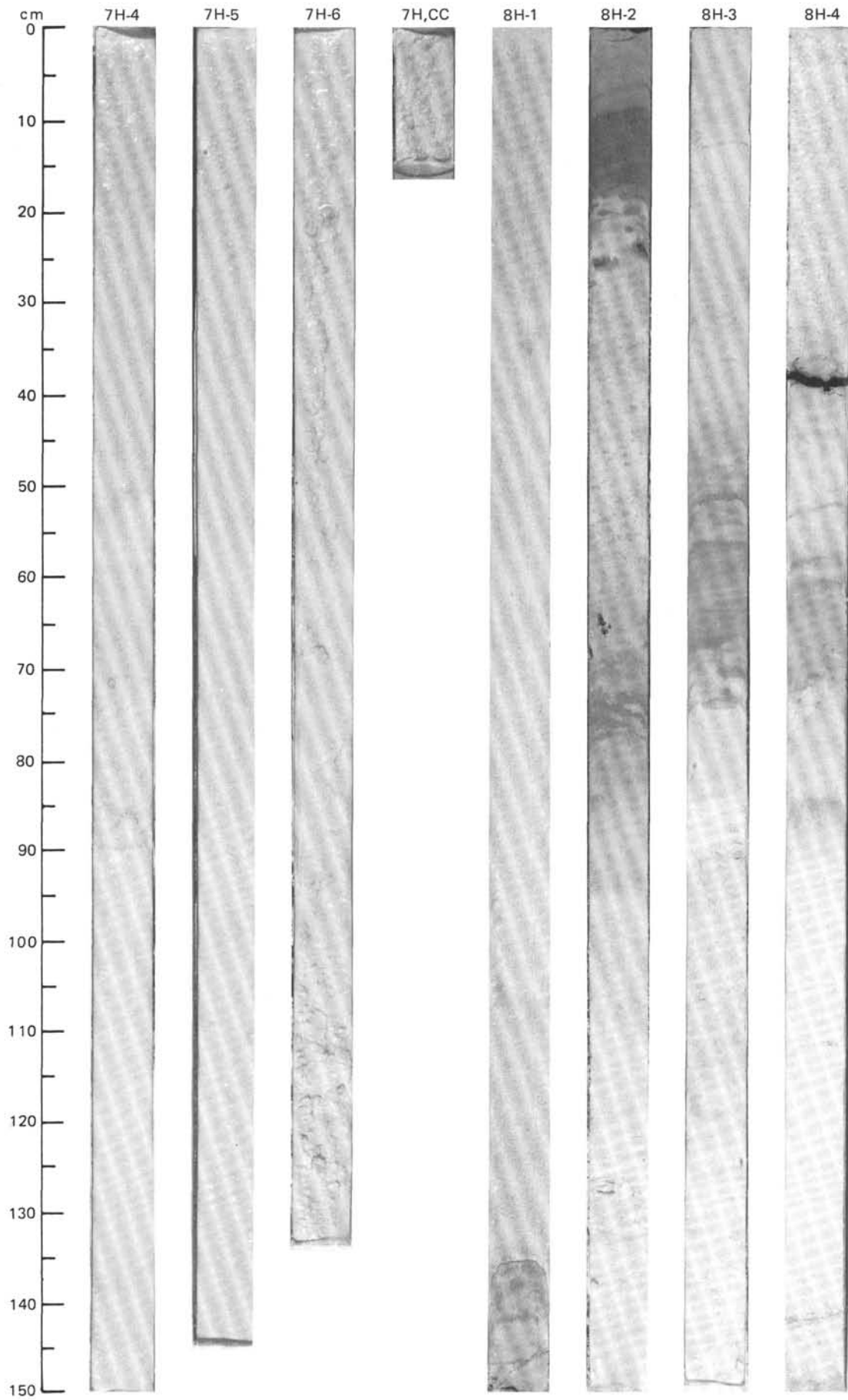


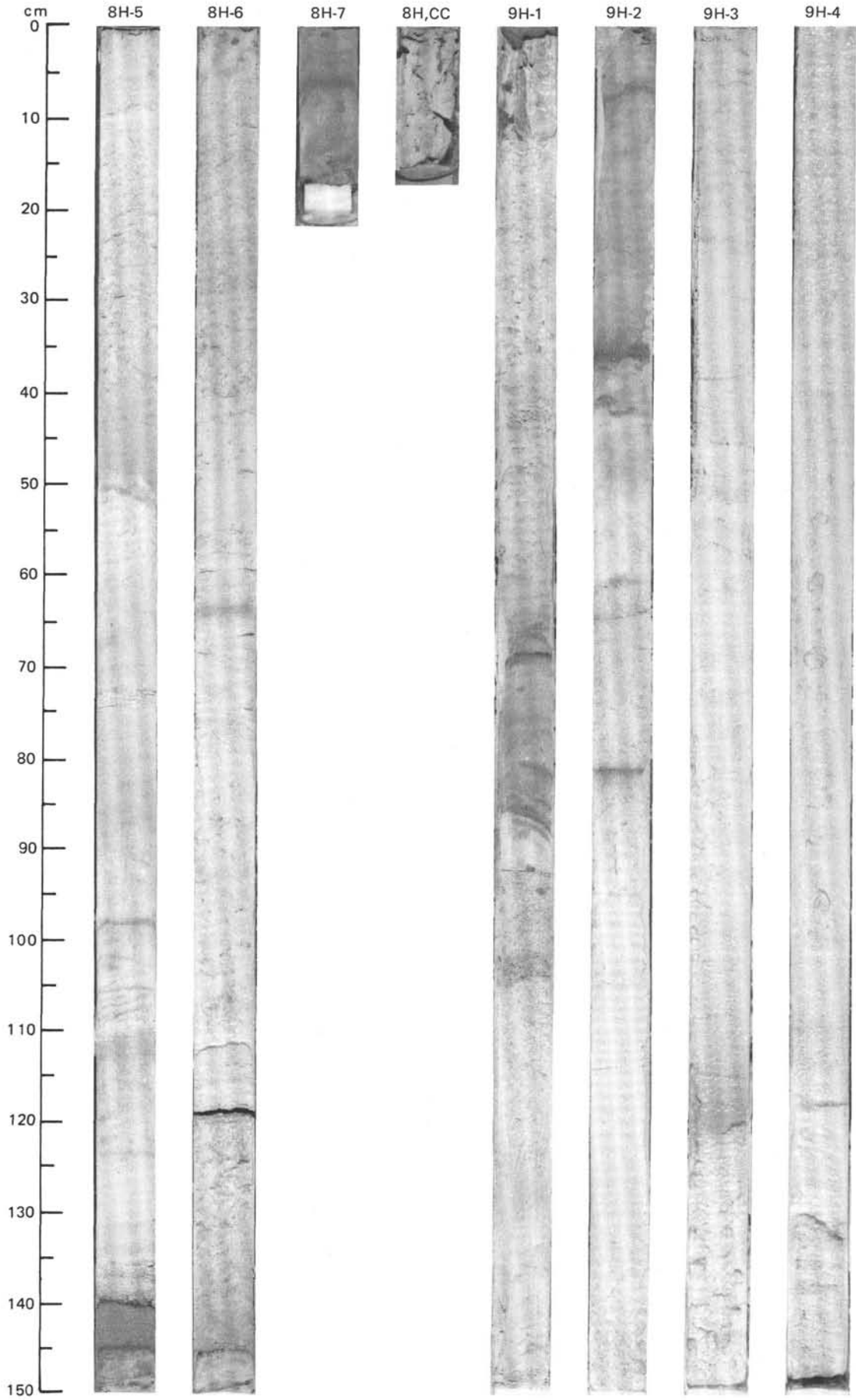
SITE 666 (HOLE A)



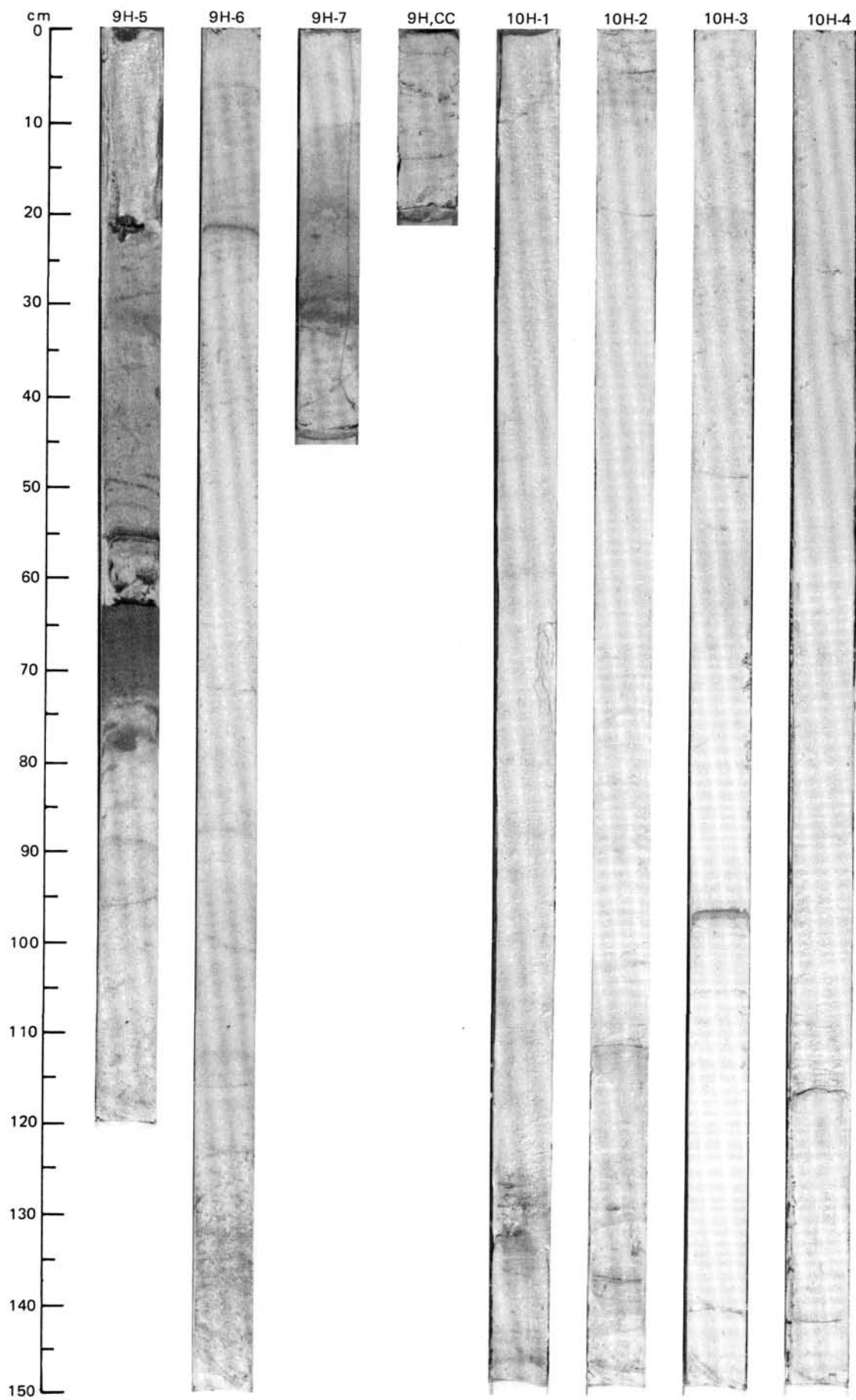


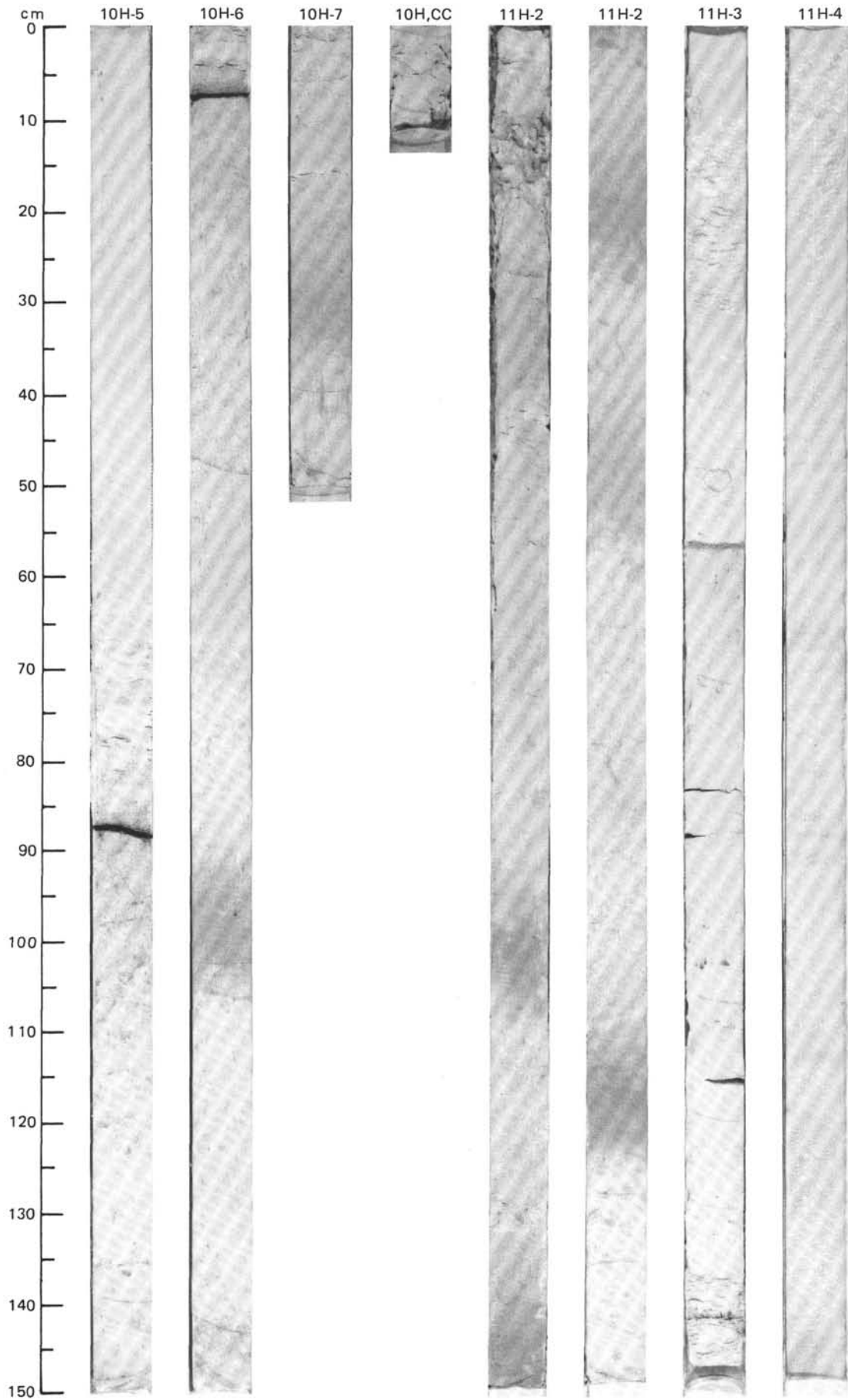
SITE 666 (HOLE A)



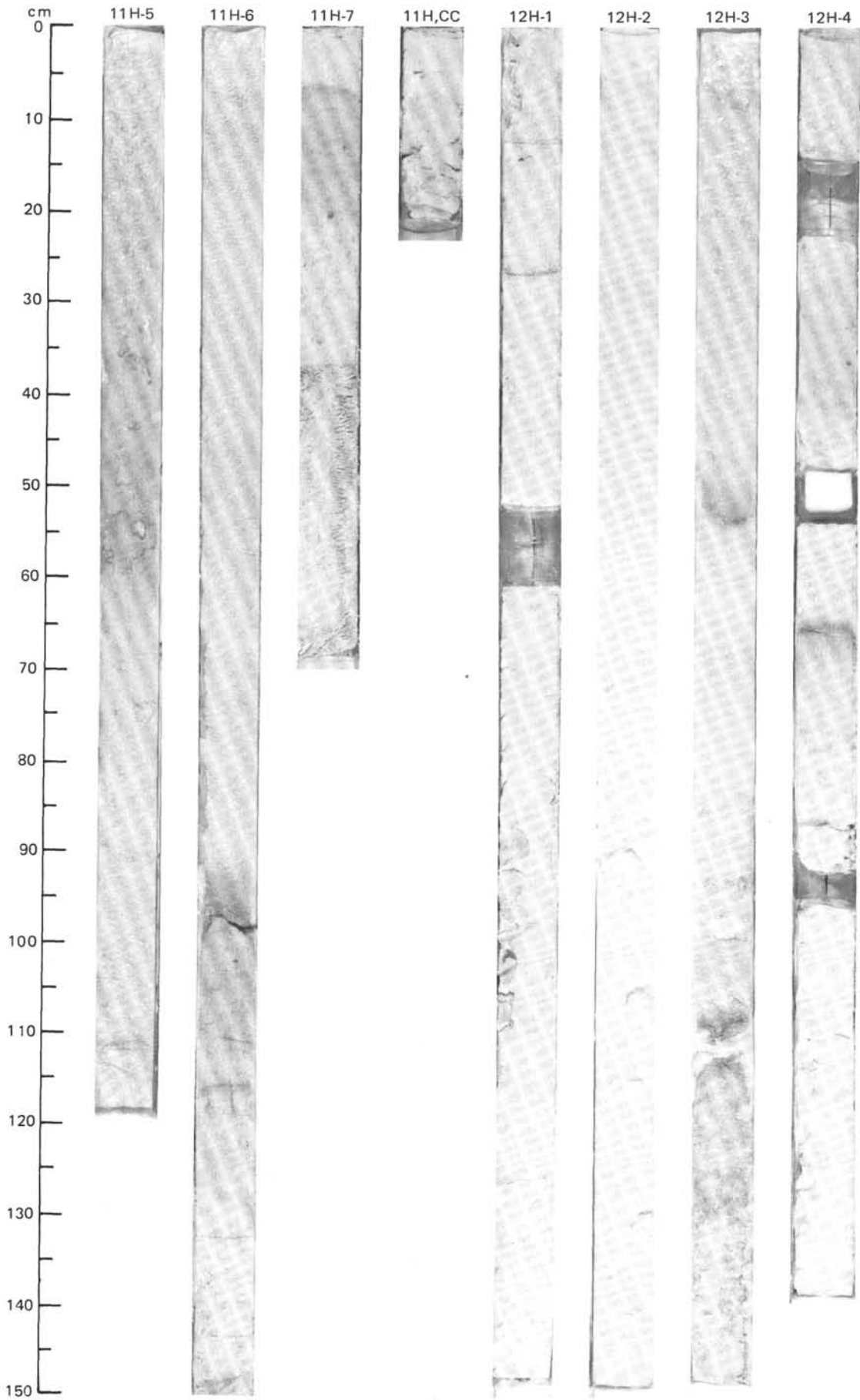


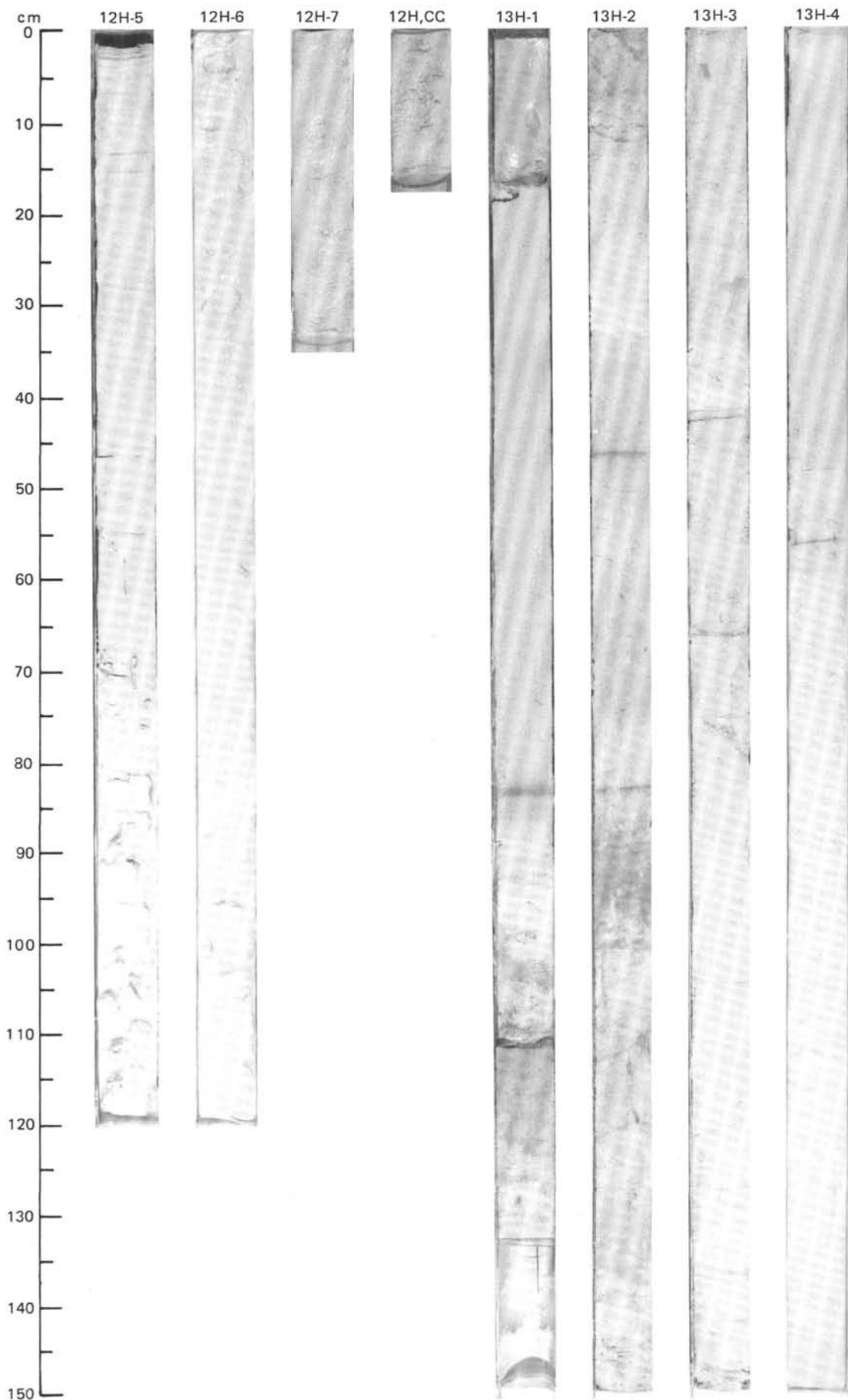
SITE 666 (HOLE A)



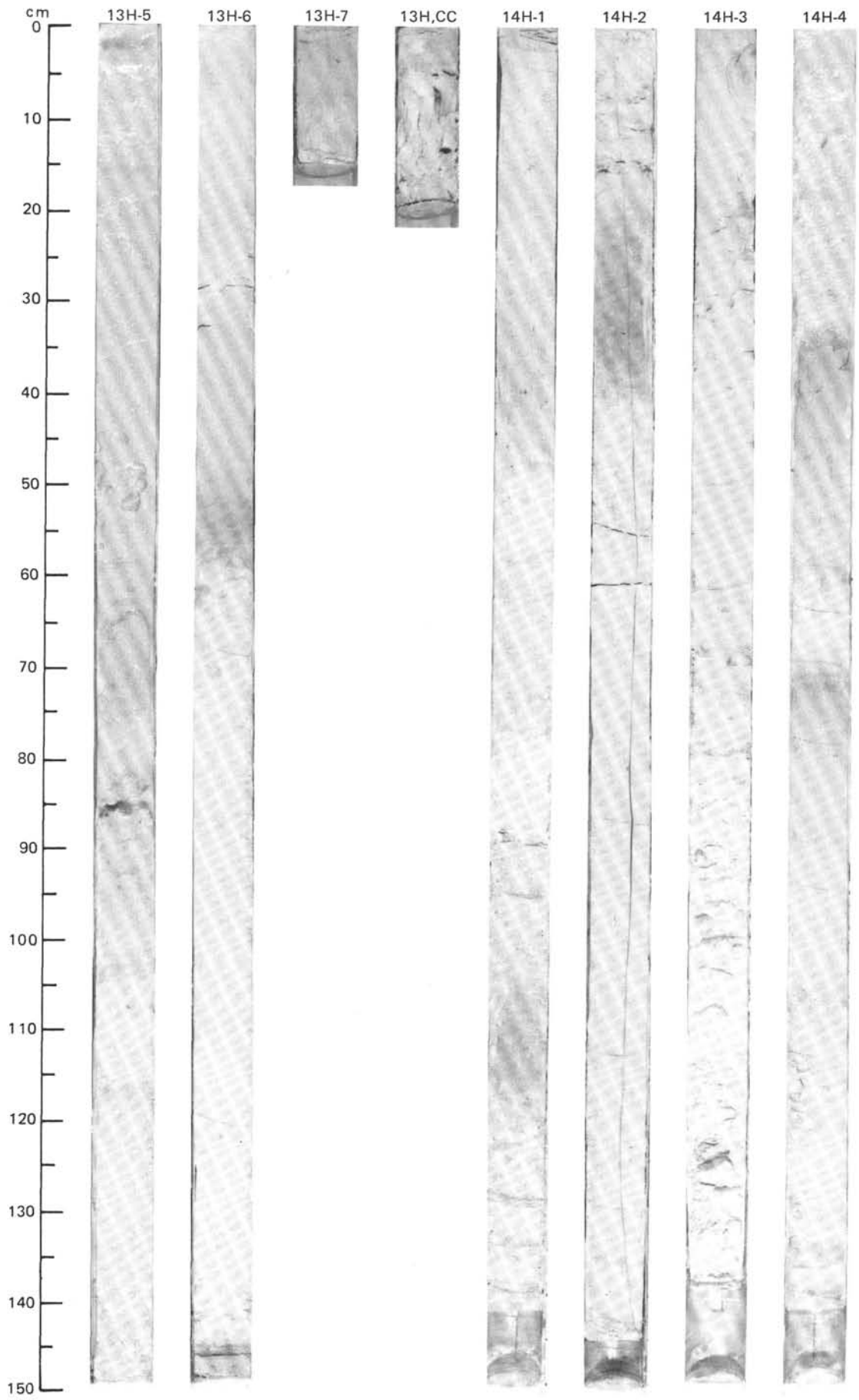


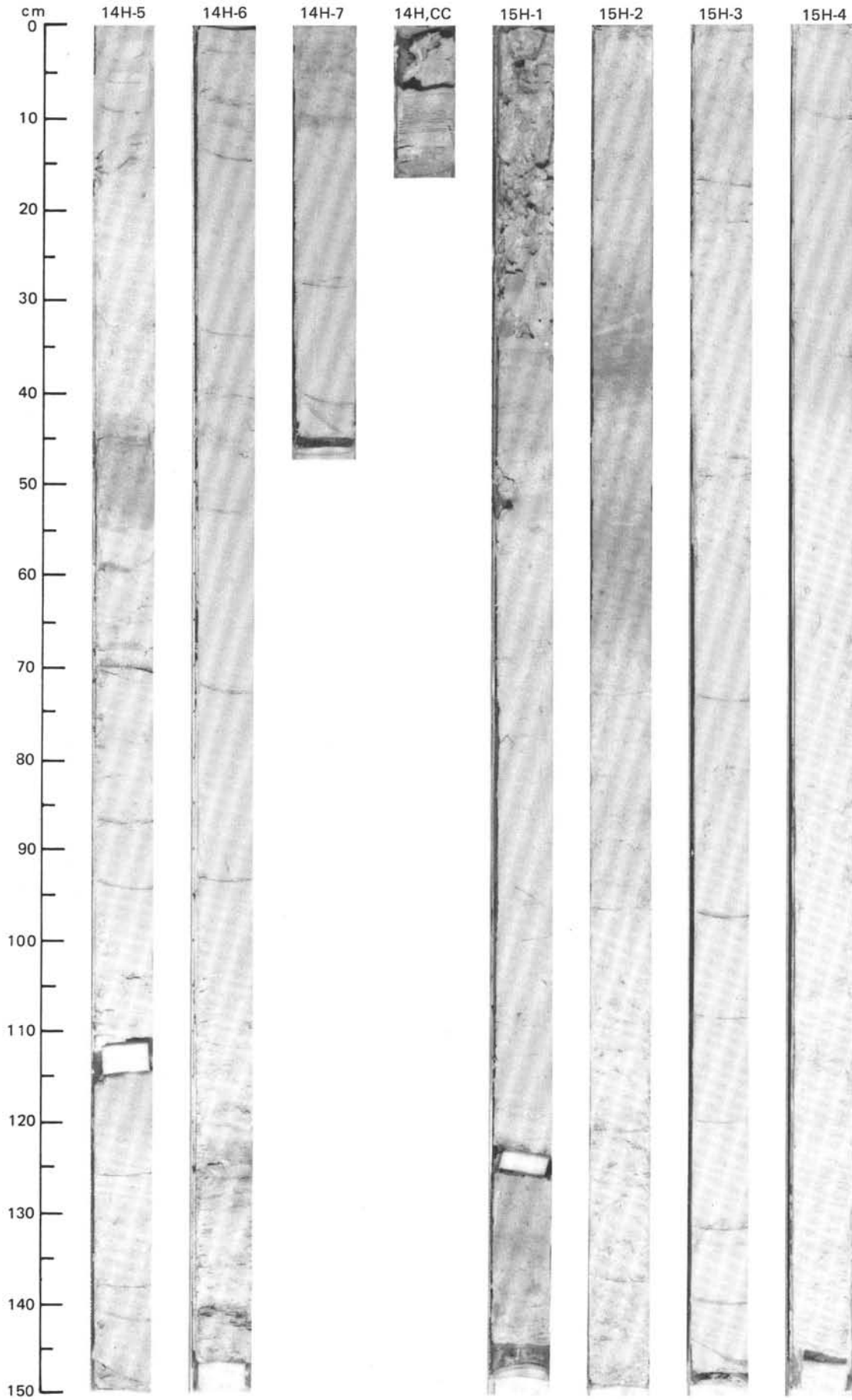
SITE 666 (HOLE A)





SITE 666 (HOLE A)





SITE 666 (HOLE A)

